

# Projector-based renormalization method (PRM) and its application to many-particle systems

Andreas Hubsch, Steffen Sykora, and Klaus W. Becker

Institut für Theoretische Physik, Technische Universität Dresden, 01062 Dresden, Germany

(Dated: February 20, 2024)

Despite the advances in the development of numerical methods analytical approaches play a key role on the way towards a deeper understanding of strongly interacting systems. In this regard, renormalization schemes for Hamiltonians represent an important new direction in the field. Among these renormalization schemes the projector-based renormalization method (PRM) reviewed here might be the approach with the widest range of possible applications: As demonstrated in this review, continuous unitary transformations, perturbation theory, non-perturbative phenomena, and quantum phase transitions can be understood within the same theoretical framework. This review starts from the definition of an effective Hamiltonian by means of projection operators that allows the evaluation within perturbation theory as well as the formulation of a renormalization scheme. The developed approach is then applied to three different many-particle systems: At first, we study the electron-phonon problem to discuss several modifications of the method and to demonstrate how phase transitions can be described within the PRM. Secondly, to show that non-perturbative phenomena are accessible by the PRM, the periodic Anderson is investigated to describe heavy-fermion behavior. Finally, we discuss the quantum phase transition in the one-dimensional Holstein model of spinless fermions where both metallic and insulating phase are described within the same theoretical framework.

## Contents

I. Introduction	1	A. Uniform description of metallic and insulating phases at half-filling	22
II. Projector-based renormalization method (PRM)	2	B. Results	23
A. Basic concepts	3	VII. Charge ordering and superconductivity in the two-dimensional Holstein model	25
B. Perturbation theory	3	A. Unified description of SC and CDW phases at half-filling	25
C. Stepwise renormalization	4	B. Results and Discussion	25
D. Generator of the unitary transformation and further approximations	5	VIII. Summary	26
E. Example: Fano-Anderson model	6	Acknowledgments	26
F. Generalized generator of the unitary transformation	7	A. Example: dimerized and frustrated spin chain	27
G. Fano-Anderson model revisited	8	References	28
III. Renormalization of the electron-phonon interaction	9	I. INTRODUCTION	
A. Frohlich's transformation	9	During the last three decades the investigation of phenomena related with strongly interacting electrons has developed to a central field of condensed matter physics. In this context, high-temperature superconductivity and heavy-fermion behavior are maybe the most important examples. It has been clearly turned out that such systems require true many-body approaches that properly take into account the dominant strong electronic correlations.	
B. Continuous transformation	10	In the past, many powerful numerical methods like exact diagonalization (1), numerical renormalization group (2), Quantum Monte-Carlo (3), the density-matrix renormalization group (4), or the dynamical mean-field theory (5) have been developed to study strongly correlated electronic systems. In contrast, only very few analytical approaches are available to tackle such systems. In this	
C. Improved renormalization scheme and BCS-gap equation	11		
D. Discussion	13		
IV. Heavy-fermion behavior in the periodic Anderson model	13		
A. Renormalization ansatz	14		
B. Generator of the unitary transformation	15		
C. Renormalization equations	15		
D. Analytical solution	16		
E. Numerical solution	17		
V. Crossover behavior in the metallic one-dimensional Holstein model	18		
A. Metallic solutions	18		
B. A diabatic case	19		
C. Intermediate case	20		
D. Anti-diabatic case	21		
E. Discussion	21		
VI. Quantum Phase transition in the one-dimensional Holstein model	22		

regard, renormalization schemes for Hamiltonians developed in the nineties of the last century (6; 7; 8) represent an important new direction in the field where renormalization schemes are implemented in the Liouville space (that is built up by all operators of the Hilbert space). Thus, these approaches can be considered as further developments of common renormalization group theory (9) that is based on a renormalization within the Hilbert space.

In this review we want to discuss the projector-based renormalization method [PRM, Ref. 10] that shares some basic concepts with the renormalization schemes for Hamiltonians mentioned above (6; 7; 8). All these approaches including the PRM generate effective Hamiltonians by applying a sequence of unitary transformations to the initial Hamiltonian of the physical system. However, there is one distinct difference between these methods: Both similarity renormalization (6; 7) and Wegner's flow equation method (8) start from a continuous formulation of the unitary transformation by means of a differential form. In contrast, the PRM is based on discrete transformations so that a direct link to perturbation theory can be provided.

This review is organized as follows:

In the next section we discuss the basic concepts of the PRM: We introduce projection operators in the Liouville space that allow the definition of an effective Hamiltonian. If these ingredients are combined with unitary transformations one can derive a new kind of perturbation theory that is not restricted to the ground-state but also allows to investigate excitations. (To illustrate this point we briefly discuss the triplet dispersion relation of a dimerized and frustrated spin chain in the Appendix.) However, this perturbation theory is not the focus of this review and can be considered as an interesting side-product of the development of the PRM, a renormalization scheme based on the same ingredients. To illustrate the method in some detail, the exactly solvable Fano-Anderson model is considered.

Improving our previous publications on the PRM, we show here the relation of the PRM to Wegner's flow equation method (8) for the first time. It turns out the latter method can be understood within the framework of the PRM by choosing a complementary unitary transformations to generate the effective Hamiltonian. For demonstration, the Fano-Anderson model is solved with this approach, too.

As a more physical example, the electron-phonon interaction is studied in Sec. III. In particular, the PRM is compared in some detail with the flow equation method (8) and the similarity transformation (6; 7). Furthermore, we introduce a possible modification of the PRM that allows to derive block-diagonal Hamiltonians, and we discuss in some detail the freedom in choosing the generator of the unitary transformation the PRM is based on. Finally, we show how phase transitions can be studied within the PRM by adding symmetry breaking fields

to the Hamiltonian.

In Sec. IV the PRM is applied to the periodic Anderson model to describe heavy-fermion behavior. Whereas the famous slave-boson mean-field theory (11; 12) obtains an effectively free system consisting of two non-interacting fermionic quasi-particles, here the periodic Anderson model is mapped onto an effective model that still takes into account electronic correlations. Thus, in principle both mixed and integral valence solution can be found. However, here we restrict ourselves to an analytical solution of the renormalization equations that is limited to the mixed valence case.

As third application of the PRM the one-dimensional Holstein model of spinless fermions is discussed. It is well known that the system undergoes a quantum phase transition from a metallic to a Peierls distorted state if the electron-phonon coupling exceeds a critical value. First, for the metallic state we discuss the crossover behavior between the adiabatic and anti-adiabatic case in Sec. V. All physical properties are shown to strongly depend on the ratio of phonon and hopping energy in the system. In Sec. VI, a unified description of the quantum phase transition is given for the one-dimensional model in the adiabatic case.

Finally, as a second example for a quantum phase transition, we discuss in Sec. VII the competition of charge ordering and superconductivity in the two-dimensional Holstein model. Based on the PRM both charge density wave and superconductivity are studied within one theoretical framework.

We summarize in Sec. VIII.

## II. PROJECTOR-BASED RENORMALIZATION METHOD (PRM)

In this section we introduce the concepts of the PRM (10) where we particularly pay attention to a general notation that is used throughout the review for all applications of the approach.

We define projection operators of the Liouville space and define an effective Hamiltonian where, in contrast to common approaches, excitations instead of states are integrated out. In this way, not only a perturbation theory is derived but also and more important a renormalization scheme (that we call PRM in the following) is established which allows to diagonalize or at least to quasi-diagonalize many-particle Hamiltonians. As an illustrative example, the exactly solvable Fano-Anderson model is discussed.

The PRM is based on a sequence of finite unitary transformations whereas Wegner's flow equations start from a continuous formulation of unitary transformations by means of a differential form. It turns out that such a continuous transformation can also be understood in the framework of the PRM if a complementary choice for the generator of the unitary transformation is used and in finitely small transformation steps are considered. To

discuss the differences between the two formulations of the PRM. In more detail, we also solve the Fano-Anderson model using the developed continuous approach.

#### A. Basic concepts

The projector-based renormalization method (PRM) (10) starts from the usual decomposition of a given many-particle Hamiltonian,

$$H = H_0 + H_1;$$

where the perturbation  $H_1$  should not contain any terms that commute with the unperturbed part  $H_0$ . Thus, the interaction  $H_1$  consists of the transitions between eigenstates of  $H_0$  with corresponding non-zero transition energies. The presence of  $H_1$  usually prevents an exact solution of the eigenvalue problem of the full Hamiltonian  $H$  so that suited approximations are necessary.

The aim is to construct an effective Hamiltonian  $H$  with a renormalized 'unperturbed' part  $H_0$ ; and a remaining 'perturbation'  $H_1$ ;

$$H = H_0 + H_1; \quad (2.1)$$

with the following properties:

- (i) The eigenvalue problem of the renormalized Hamiltonian  $H_0$  is diagonal

$$H_0 |j\rangle = E_n |j\rangle$$

with  $n$ -dependent eigenvalues  $E_n$  and eigenvectors  $|j\rangle$ .

- (ii) The effective Hamiltonian  $H$  is constructed in such a way so that (measured with respect to  $H_0$ ) all non-diagonal contributions with transition energies larger than some cutoff energy vanish.

- (iii)  $H$  has the same eigenvalues as the original Hamiltonian  $H$ .

The eigenvalue problem of  $H_0$  is crucial for the construction of  $H$  because it can be used to define projection operators,

$$P = \sum_{m,n} |j\rangle \langle m| \delta_{jm} \delta_{jn} \quad (2.2)$$

$$Q = 1 - P; \quad (2.3)$$

Note that neither  $|j\rangle$  nor  $\langle m|$  need to be low- or high-energy eigenstates of  $H_0$ .  $P$  and  $Q$  are superoperators acting on operators  $A$  of the Hilbert space of the system. Thus,  $P$  and  $Q$  can be interpreted as projection operators of the Liouville space that is built up by all operators of the Hilbert space.  $P$  projects on those

parts of an operator  $A$  which only consist of transition operators  $|j\rangle \langle m|$  with energy differences  $|E_n - E_m|$  less than a given cutoff, whereas  $Q$  projects onto the high-energy transitions of  $A$ .

In terms of the projection operators  $P$  and  $Q$  the property of  $H$  to allow no transitions between the eigenstates of  $H_0$  with energies larger than reads

$$H = P H \quad \text{or} \quad Q H = 0; \quad (2.4)$$

For an actual construction of the effective Hamiltonian we now assume that the effective Hamiltonian  $H$  can be obtained from the original Hamiltonian by a unitary transformation,

$$H = e^X H e^{-X}; \quad (2.5)$$

which shall automatically guarantee that condition (iii) above is fulfilled.

In the following the evaluation of the effective Hamiltonian (2.5) is done in two ways: At first a perturbative treatment is derived. After that we develop a much more sophisticated renormalization where we interpret the unitary transformation of Eq. (2.5) as a sequence of small transformations. The projector-based perturbation theory discussed in the next subsection is important for the understanding of the renormalization scheme derived later. However, the main focus of this review is the PRM.

#### B. Perturbation theory

In the following we evaluate the effective Hamiltonian  $H$  in perturbation theory. For this purpose the effective Hamiltonian  $H$  from Eqs. (2.4) and (2.5) is simplified in a crucial point: The projection operators are now defined with respect to the eigenvalue problem of the unperturbed part of the original Hamiltonian  $H_0$ ,

$$H_0 |j\rangle = E_n |j\rangle$$

Thus, these projection operators differ from the formerly defined projectors  $P$  and  $Q$  and can be written as follows

$$P = \sum_{m,n} |j\rangle \langle m| \delta_{jm} \delta_{jn} \quad (2.6)$$

$$Q = 1 - P; \quad (2.7)$$

The renormalized Hamiltonian  $H$  is now obtained from the unitary transformation (2.5),

$$H = P H = e^X H e^{-X};$$

where  $X$  is the generator of this transformation. To find  $X$ , we employ the modified condition (2.4): All matrix elements of  $H$  for transitions with energies larger than vanish, i.e.

$$Q H = 0 \quad (2.8)$$

First we expand  $H$  with respect to  $X$ ,

$$H = H_0 + [X; H_0] + \frac{1}{2!} [X; [X; H_0]] + \frac{1}{3!} [X; [X; [X; H_0]]] + \dots \quad (2.9)$$

and assume that the generator  $X$  can be written as a power series in the interaction  $H_1$ ,

$$X = X^{(1)} + X^{(2)} + X^{(3)} + \dots \quad (2.10)$$

Thus inserting (2.10) in Eq. (2.9), the effective Hamiltonian  $H$  can be rewritten as a power series in the interaction  $H_1$

$$H = H_0 + H_1 + \frac{1}{2!} [X^{(1)}; H_0] + \frac{1}{2!} [X^{(1)}; H_1] + \frac{1}{2!} [X^{(2)}; H_0] + \frac{1}{2!} [X^{(1)}; [X^{(1)}; H_0]] + O(H_1^3) \quad (2.11)$$

The contributions  $X^{(n)}$  to the generator of the unitary transformation can successively be determined by employing Eq. (2.8). One finds

$$Q X^{(1)} = \frac{1}{L_0} Q H_1; \quad (2.12)$$

$$Q X^{(2)} = \frac{1}{2L_0} Q ([X^{(1)}; H_1]); \frac{1}{L_0} Q H_1 \quad (2.13)$$

$$\frac{1}{L_0} Q ([X^{(1)}; H_1]); \frac{1}{L_0} Q H_1 :$$

Here,  $L_0$  is the Liouville operator of the unperturbed Hamiltonian  $H_0$  which is defined by  $L_0 A = [H_0; A]$  for any operator variable  $A$ .

As one can see from (2.12) and (2.13), no information about the low-energy part  $P X$  of the generator  $X$  can be deduced from (2.8). Therefore, we set for simplicity

$$P X = P X^{(1)} = P X^{(2)} = \dots = 0 \quad (2.14)$$

Inserting Eqs. (2.12), (2.13), and (2.14) into the power series (2.11) for  $H$ , the desired perturbation theory is found,

$$H = H_0 + P H_1 + \frac{1}{2} P ([X^{(1)}; H_1]); \frac{1}{L_0} Q H_1 + P ([X^{(1)}; H_1]); \frac{1}{L_0} Q H_1 + O(H_1^3); \quad (2.15)$$

which can easily be extended to higher order terms. Note that the correct size dependence of the Hamiltonian is automatically guaranteed by the commutators in Eq. (2.15). The limit  $\hbar \rightarrow 0$  is of particular interest because in this case the complete interaction  $H_1$  is integrated out.

Usual perturbation theory derives effective Hamiltonians that are only valid for a certain range of the system's Hilbert space. In contrast,  $H$ , as derived above, has no limitations with respect to the Hilbert space so that it

can also be used to study excited states. To illustrate this important aspect of our projector-based perturbation theory, we discuss the dimerized and frustrated spin chain in the appendix.

At this point we would like to note that Eq. (2.15) can also be derived in a different way. It turns out that  $X^{(2)}$  is only needed to fulfill the requirement  $H = P H$  if we restrict ourselves to second order perturbation theory. Thus, in this case  $X^{(2)}$  can be set to 0 if the projector  $P$  is applied to the right hand side of Eq. (2.11),

$$H = H_0 + P H_1 + P \frac{1}{2!} [X^{(1)}; H_0] + P \frac{1}{2!} [X^{(1)}; H_1] + \frac{1}{2!} P [X^{(1)}; [X^{(1)}; H_0]] + \dots \quad (2.16)$$

It is easy to prove that Eq. (2.16) again leads to the result Eq. (2.15) if (2.14) and (2.12) is used.

In Appendix A, the developed perturbation theory (2.15) is applied to the dimerized and frustrated spin chain where ground-state energy and triplet dispersion relation have been calculated.

A perturbation theory based on Wegner's flow equations (8), that also allows a description of the complete Hilbert space, has been derived in Refs. 13 and 14. However, this approach requires an equidistant spectrum of the unperturbed Hamiltonian  $H_0$ . In contrast, the perturbation theory presented here can be applied to systems with arbitrary Hilbert space, and has similarities to a cumulant approach to effective Hamiltonians (15).

### C. Stepwise renormalization

In the previous subsection the effective Hamiltonian  $H$  as defined by Eqs. (2.4) and (2.5) has been evaluated within a new kind of perturbation theory. However, if the unitary transformation (2.5) is interpreted as a sequence of unitary transformations a renormalization scheme can be developed based on the same definition of the effective Hamiltonian. Because again the projection operators  $P$  and  $Q$  play a key role we call the derived method (10) projector-based renormalization method (PRM).

Let us start from a renormalized Hamiltonian  $H = H_0 + H_1$ , that has been obtained after all transitions with energy differences larger than  $\hbar\omega$  have already been integrated out. Of course,  $H_0$  and  $H_1$  will differ from the original  $H_0$  and  $H_1$ . Furthermore, we assume  $H$  has the properties (i)-(iii) proposed in subsection II A.

Now we want to eliminate all excitations within the energy range between  $\hbar\omega$  and a smaller new energy cutoff  $\hbar\omega'$ . Thereby we use a unitary transformation,

$$H(\omega') = e^{X'} H e^{-X'}; \quad (2.17)$$

so that the effective Hamiltonian  $H_{\text{eff}}$  has the same eigenspectrum as the Hamiltonian  $H_0$ . Note that the generator  $X_1$  needs to be chosen anti-Hermitian,  $X_1^\dagger = -X_1$ , to ensure that  $H_{\text{eff}}$  is Hermitian when  $H_0$  was Hermitian before. To find an appropriate generator  $X_1$  of the unitary transformation, we employ the condition that  $H_{\text{eff}}$  has (with respect to  $H_0$ ) only vanishing matrix elements for transitions with energies larger than  $\Delta$ , i.e.  $Q H_{\text{eff}} = 0$ . Similarly, also

$$Q (H_0 - E_0) = 0 \quad (2.18)$$

must be fulfilled, where  $Q$  is now defined with respect to the excitations of  $H_0$ .

In principle, there are two strategies to evaluate Eqs. (2.17) and (2.18): The first uses perturbation theory as derived in subsection II.B. In this case  $H_{\text{eff}}$  can be written as

$$\begin{aligned} H_{\text{eff}} &= \\ &= H_0 + P (H_1 + P [X_1; H_0]) \\ &\quad + P [X_1; H_1] \\ &\quad + \frac{1}{2} P [X_1; [X_1; H_0]] + O(H_1^3); \end{aligned} \quad (2.19)$$

The generator  $X_1$  has to be chosen corresponding to Eq. (2.12),

$$Q X_1 = \frac{1}{L_0} Q H_1 + \dots \quad (2.20)$$

For details of the derivation we refer to subsection II.B. This approach has been successfully applied to the electron-phonon interaction to describe superconductivity (20).

Alternatively, one can also start from an appropriate ansatz for the generator in order to calculate  $H_{\text{eff}}$  in a non-perturbative manner (21). An ansatz for the generator with the same operator structure as Eq. (2.20) is often a very good choice. This approach has been applied to the periodic Anderson model to describe heavy-fermion behavior (21; 22).

It turns out that the second strategy has the great advantage to successfully prevent diverging renormalization contributions. However, in both cases, Eqs. (2.17) and (2.18) describe a renormalization step that lowers the energy cutoff of the effective Hamiltonian from  $\Delta$  to  $\Delta/2$ . Consequently, difference equations for the Hamiltonian  $H_{\text{eff}}$  can be derived, and the resulting equations for the dependence of the parameters of the Hamiltonian are called renormalization equations. By starting from the original model  $H = H_0$  the Hamiltonian is renormalized by reducing the cutoff in steps  $\Delta/2$ . The limit  $\Delta \rightarrow 0$  provides the desired effective Hamiltonian  $H_{\text{eff}} = H_0$  without any interaction. Note that the results strongly depend on the parameters of the original Hamiltonian  $H_0$ .

#### D. Generator of the unitary transformation and further approximations

It turns out that the generator  $X_1$  of the unitary transformation is not yet completely determined by Eqs. (2.17) and (2.18). Instead, the low-energy excitations included in  $X_1$ , namely the part  $P (H_1 + P [X_1; H_0])$ , can be chosen arbitrarily. The result of the renormalization scheme should not depend on the particular choice of  $P (H_1 + P [X_1; H_0])$  as long as all renormalization steps are performed without approximations. However, approximations will be necessary for practically all interacting systems of interest so the choice  $P (H_1 + P [X_1; H_0])$  becomes relevant. If  $P (H_1 + P [X_1; H_0]) = 0$  is chosen the minimal transformation is performed to match the requirement (2.18). Such an approach of "minimal" transformations avoid errors caused by approximations necessary for every renormalization step as much as possible. Note that in order to derive the expression (2.19) this choice of  $P (H_1 + P [X_1; H_0])$  was used. However, in particular cases a non-zero choice for  $P (H_1 + P [X_1; H_0])$  might help to circumvent problems in the evaluation of the renormalization equations.

In general, new interaction terms can be generated in every renormalization step. This might allow the investigation of competing interactions which naturally emerge within the renormalization procedure. However, actual calculations require a closed set of renormalization equations. Thus, often a factorization approximation has to be performed in order to trace back complicated operators to terms already appearing in the renormalization ansatz. Consequently, derived effective Hamiltonians might be limited in their possible applications if important operators have not been appropriately included in the renormalization scheme.

If a factorization approximation needs to be performed the obtained renormalization equations will contain expectation values that must be calculated separately. In principle, these expectation values are defined with respect to  $H_{\text{eff}}$  because the factorization approximation was employed for the renormalization step that transformed  $H_0$  to  $H_{\text{eff}}$ . However,  $H_{\text{eff}}$  still contains interactions that prevent a straight evaluation of required expectation values. The easiest way to circumvent this difficulty is to neglect the interactions and to use the diagonal unperturbed part  $H_0$  instead of  $H_{\text{eff}}$  for the calculation of the expectation values. This approach has been successfully applied to the Holstein model to investigate single-particle excitations and phonon softening (23). However, it turns out that often the interaction term in  $H_{\text{eff}}$  is crucial for a proper calculation of the required expectation values. Thus, usually a more involved approximation has been used that neglects the dependence of the expectation values but includes interaction effects by calculating the expectation values with respect to the full Hamiltonian  $H_{\text{eff}}$  instead of  $H_0$ . In this case, the renormalization equations need to be solved in a self-consistent manner.

ner because they depend on expectation values defined with respect to the full Hamiltonian  $H$  which are not known from the very beginning but can be determined from the fully renormalized (and diagonal) Hamiltonian  $H^* = \lim_{\lambda \rightarrow 0} H$ .

There exist two ways to calculate expectation values of the full Hamiltonian from the renormalized Hamiltonian. The first one is based on the free energy that can be calculated either from the original model  $H$  or the renormalized Hamiltonian  $H^*$ ,

$$F = -\frac{1}{\beta} \ln \text{Tr} e^{-\beta H} = -\frac{1}{\beta} \ln \text{Tr} e^{-\beta H^*};$$

because  $H^*$  is obtained from  $H$  by unitary transformations. The desired expectation values can then be determined from the free energy by functional derivatives. This approach has advantages as long as the derivatives can be evaluated analytically as, for example, in Refs. 20 and 21.

The second way to calculate expectation values of the full Hamiltonian employs unitarity for any operator variable  $A$ ,

$$\langle A \rangle = \frac{\text{Tr} A e^{-\beta H}}{\text{Tr} e^{-\beta H}} = \frac{\text{Tr} \tilde{A} e^{-\beta H^*}}{\text{Tr} e^{-\beta H^*}};$$

where we defined  $\tilde{A} = \lim_{\lambda \rightarrow 0} A$ . Thus, additional renormalization equations need to be derived for the required operator variables  $A$  where the same sequence of unitary transformations has to be applied to the operator variable  $A$  as to the Hamiltonian  $H$ .

#### E. Example: Fano-Anderson model

In this subsection we want to illustrate the PRM discussed above by considering an exactly solvable model, namely the Fano-Anderson model (24; 25),

$$\begin{aligned} H &= H_0 + H_1; \\ H_0 &= \sum_{k,m} \epsilon_f^y f_{k,m}^\dagger f_{k,m} + \sum_{k,m} \epsilon_k^y c_{k,m}^\dagger c_{k,m}; \\ H_1 &= \sum_{k,m} V_k f_{k,m}^\dagger c_{k,m} + \sum_{k,m} c_{k,m}^\dagger f_{k,m}; \end{aligned} \quad (2.21)$$

The Hamiltonian (2.21) describes dispersion-less  $f$  electrons interacting with conduction electrons where all correlation effects are neglected.  $k$  denotes the wave vector, and the one-particle energies are measured with respect to the chemical potential. Both types of electrons are assumed to have the same orbital index  $m$  with values  $1, \dots, f$ . The model (2.21) is easily diagonalized,

$$H = \sum_{k,m} \epsilon_k^{(y)} f_{k,m}^\dagger f_{k,m} + \sum_{k,m} \epsilon_k^{(c)} c_{k,m}^\dagger c_{k,m}; \quad (2.22)$$

where  $\epsilon_k^{(y)}$  and  $\epsilon_k^{(c)}$  are given by linear combinations of the original fermionic operators  $c_{k,m}^y$  and  $f_{k,m}^y$ ,

$$\epsilon_k^{(y)} = u_k f_{k,m}^y + v_k c_{k,m}^y; \quad (2.23)$$

$$\epsilon_k^{(c)} = v_k f_{k,m}^y + u_k c_{k,m}^y; \quad (2.24)$$

$$\begin{aligned} u_k &= \frac{1}{2} \left( 1 + \frac{\epsilon_k^f - \epsilon_k^c}{W_k} \right); \\ v_k &= \frac{1}{2} \left( 1 + \frac{\epsilon_k^c - \epsilon_k^f}{W_k} \right); \end{aligned}$$

Here, we defined  $W_k = \frac{1}{4} (\epsilon_k^f - \epsilon_k^c)^2 + 4V_k^2$ , and the eigenvalues of  $H$  are given by

$$\epsilon_k^{(y)} = \frac{\epsilon_k^f + \epsilon_k^c}{2} \pm \frac{1}{2} W_k; \quad (2.25)$$

In the following, we want to apply the PRM as introduced above to the Fano-Anderson model (2.21) where we mainly use the formulation of Ref. (21). The goal is to integrate out the hybridization term  $H_1$  so that we finally obtain an effectively free model. Therefore, having in mind the exact solution of the model, we make the following renormalization ansatz:

$$\begin{aligned} H &= H_0 + H_1; \\ H_0 &= \sum_{k,m} \epsilon_k^f f_{k,m}^\dagger f_{k,m} + \sum_{k,m} \epsilon_k^c c_{k,m}^\dagger c_{k,m}; \\ H_1 &= \sum_{k,m} V_k f_{k,m}^\dagger c_{k,m} + \sum_{k,m} c_{k,m}^\dagger f_{k,m}; \end{aligned} \quad (2.26)$$

Note that  $V_k$  includes a cutoff function in order to ensure that the requirement  $\lim_{k \rightarrow 0} V_k = 0$  is fulfilled.

In the next step we want to eliminate excitations with energies within the energy shell between  $\epsilon_f$  and  $\epsilon_c$  by means of an unitary transformation similar to (2.17). By inspecting the perturbation expansion corresponding to subsection II B, the generator of the unitary transformation must have the following form:

$$X = \sum_{k,m} A_k(\epsilon; \epsilon_f) f_{k,m}^\dagger c_{k,m} - \sum_{k,m} A_k(\epsilon; \epsilon_c) c_{k,m}^\dagger f_{k,m}; \quad (2.27)$$

where the parameters  $A_k(\epsilon; \epsilon)$  need to be properly determined so that Eq. (2.18) is fulfilled. To evaluate the transformation (2.17), we now consider the transformations of the operators appearing in the renormalization ansatz (2.26). For example, we obtain

$$\begin{aligned} e^{X^\dagger} c_{k,m}^\dagger c_{k,m} e^X &= c_{k,m}^\dagger c_{k,m} \\ &= \frac{1}{2} \cos[2A_k(\epsilon; \epsilon_f)] c_{k,m}^\dagger c_{k,m} + \frac{1}{2} \sin[2A_k(\epsilon; \epsilon_f)] f_{k,m}^\dagger c_{k,m} \\ &\quad + \frac{1}{2} \cos[2A_k(\epsilon; \epsilon_c)] c_{k,m}^\dagger c_{k,m} + \frac{1}{2} \sin[2A_k(\epsilon; \epsilon_c)] f_{k,m}^\dagger c_{k,m}; \end{aligned}$$

Here it is important to notice that due to the fermionic anti-commutator relations the different  $k$  are not coupled with each other. Very similar transformations can also be found for  $f_{km}^y f_{km}$  and  $f_{km}^y c_{km} + c_{km}^y f_{km}$ . Inserting these transformations into (2.17) leads to the following renormalization equations:

$$\begin{aligned} u_{k;(\cdot)}^f &= u_{k;(\cdot)}^f \\ &= \frac{1}{2} \cos[2A_k(\cdot)] \lg u_{k;(\cdot)}^c + V_{k;(\cdot)} \sin[2A_k(\cdot)]; \end{aligned} \quad (2.28)$$

$$u_{k;(\cdot)}^c = u_{k;(\cdot)}^c : \quad (2.29)$$

Now we need to determine the parameters  $A_k(\cdot)$ . For this purpose we employ the condition (2.18): First, from  $Q(\cdot)H(\cdot) = 0$  we conclude  $V_{k;(\cdot)} = u_{k;(\cdot)}^f$ , where we have defined  $u_{k;(\cdot)}^f = J_{k;(\cdot)}^f u_{k;(\cdot)}^c$ . Moreover, from  $Q(\cdot)H(\cdot) = 0$  we find

$$\begin{aligned} \tan[2A_k(\cdot)] &= \\ &= \frac{1}{u_{k;(\cdot)}^f} \frac{2V_{k;(\cdot)}}{u_{k;(\cdot)}^c} \end{aligned} \quad (2.30)$$

which shows that also  $A_k(\cdot)$  contains the cutoff factor  $u_{k;(\cdot)}^f$ . Note that in the expression (2.30) the low excitation-energy part of the generator was chosen to be zero  $P(\cdot)X_{k;(\cdot)} = 0$ . As one can see from Eqs. (2.28)–(2.30), the renormalization of the parameters of a given  $k$  is not affected by other  $k$  values. Furthermore, it is important to notice that  $J_{k;(\cdot)}^f u_{k;(\cdot)}^c$ . Consequently, each  $k$  value is renormalized only once during the renormalization procedure eliminating excitations from large to small values. Such a steplike renormalization allows an easy solution of the renormalization equations (2.28)–(2.30) where  $\cdot$  is replaced by the cutoff of the original model and we set  $\cdot = 0$ . Here, one needs to consider that the parameter  $A_k$  changes its sign if the difference  $u_f - u_k$  changes its sign. Thus, we find the following renormalized Hamiltonian

$$H^* = \lim_{\cdot \rightarrow 0} H = \sum_{k,m} u_k^f f_{km}^y f_{km} + u_k^c c_{km}^y c_{km}; \quad (2.31)$$

where the renormalized energies are given by

$$u_k^f = \frac{u_f + u_k}{2} + \frac{\text{sgn}(u_f - u_k)}{2} W_{k;(\cdot)}; \quad (2.32)$$

$$u_k^c = \frac{u_f + u_k}{2} - \frac{\text{sgn}(u_f - u_k)}{2} W_{k;(\cdot)}; \quad (2.33)$$

The results of the renormalization and the diagonalization are completely comparable for physical accessible

quantities like quasiparticle energies [compare (2.25) with Eqs. (2.32) and (2.33)] or expectation values. However, there is also an important difference between the two approaches: Whereas the eigenmodes  $y_{km}$  and  $y_{km}$  of the diagonalized Hamiltonian (2.22) change their character as function of the wave vector  $k$  [compare (2.23) and (2.24)], the operators  $f_{km}^y$  and  $c_{km}^y$  of  $H^*$  remain  $f$ -like and  $c$ -like for all  $k$  values. In return, the quasiparticle energies  $u_k^f$  and  $u_k^c$  show a steplike behavior as function of  $k$  at  $u_f - u_k = 0$  so that the deviations from the original one-particle energies  $u_f$  and  $u_k$  remain relatively small for all  $k$  values.

## F. Generalized generator of the unitary transformation

As already mentioned in subsection IID, the low-energy excitations included in the generator  $X_{k;(\cdot)}$  of the unitary transformation (2.17) can be chosen arbitrarily, i.e.  $P(\cdot)X_{k;(\cdot)}$  is not determined by the condition (2.18).

In the previous subsection an approach of "minimal" transformations has been applied to the Fano-Anderson model where  $P(\cdot)X_{k;(\cdot)}$  is set to zero. However, in the following we want to demonstrate that it is also possible to take advantage of this freedom to choose the generator  $X_{k;(\cdot)}$  and to derive a continuous version of the PRM. As it will turn out in Sec. III B the PRM can also be connected to Wegner's flow equation method (8).

By allowing a nonzero part  $P(\cdot)X_{k;(\cdot)} \neq 0$  the generator  $X_{k;(\cdot)}$  of the unitary transformation (2.17) can be written as follows

$$X_{k;(\cdot)} = P(\cdot)X_{k;(\cdot)} + Q(\cdot)X_{k;(\cdot)} \quad (2.34)$$

Here the part  $Q(\cdot)X_{k;(\cdot)}$  ensures that Eq. (2.18),  $Q(\cdot)H(\cdot) = 0$ , is fulfilled. Note however, one may also choose the remaining part  $P(\cdot)X_{k;(\cdot)}$  in such a way that it almost completely integrates out all the interactions before the cutoff energy approaches their corresponding transition energies.

As it will be discussed in Sec. III in more detail, the flow equation method (8) and the PRM (in its minimal form) take advantage of the freedom to choose the generator of the unitary transformation in a very different way. In the PRM, the low transition-energy projection part of the generator,  $PX_{k;(\cdot)}$ , is set to zero for convenience. The flow equation approach instead uses exactly this part to eliminate the interaction.

Even though the PRM resembles the similarity transformation (6; 7) and Wegner's flow equation method (8) in some aspects there is an important difference: The latter two methods start from continuous transformations in differential form. This has the advantage that one can use available computer subroutines to solve the differential flow equations. In contrast, the PRM is based on

discrete transformations which lead to coupled difference equations. The advantage of the PRM is to provide a direct link to perturbation theory (as already discussed in subsection IIB). Moreover, the stepwise renormalization of the PRM allows a unified treatment on both sides of a quantum phase transition (see for example Sec. VI) which seems not to be possible in the flow equation method. However, as we show in the following the idea of continuous unitary transformations can also be implemented in the framework of the PRM.

#### G. Fano-Anderson model revisited

Now we want to demonstrate that the freedom in choosing the generator of the unitary transformation can be employed in order to derive a continuous renormalization scheme within the framework of the PRM. As an example we again discuss the Fano-Anderson model.

As already discussed, the part  $P(\epsilon)X_{k;}$  of the generator  $X_{k;}$  of the unitary transformation is not fixed by the PRM. In the former treatment of the Fano-Anderson model in subsection IIE we had chosen  $P(\epsilon)X_{k;} = 0$  for simplicity. In the following we want to take advantage of this freedom in a different way.

According to Eq. (2.27), the generator of the Fano-Anderson model is given by

$$X_{k;} = \sum_{k \neq m} A_k(\epsilon; \epsilon) f_{km}^\dagger c_{km} - \sum_{k \neq m} \tilde{A}_k(\epsilon; \epsilon) f_{km}^\dagger c_{km}$$

where the most general form of  $A_k(\epsilon; \epsilon)$  can be written as

$$A_k(\epsilon; \epsilon) = A_k^0(\epsilon; \epsilon) \epsilon_{k;}[1 - \epsilon_{k;}] + A_k^0(\epsilon; \epsilon) \epsilon_{k;}\epsilon_{k;}: \quad (2.35)$$

Here, the renormalization contributions related with  $P(\epsilon)X_{k;}$  and  $Q(\epsilon)X_{k;}$  are described by the parameters  $A_k^0(\epsilon; \epsilon)$  and  $A_k^0(\epsilon; \epsilon)$ , respectively.

A possible choice for  $A_k^0(\epsilon; \epsilon)$  is

$$A_k^0(\epsilon; \epsilon) = \frac{\epsilon_{k;}^\dagger \epsilon_{k;} V_{k;}}{\epsilon_{k;}^\dagger \epsilon_{k;}}: \quad (2.36)$$

Of course, there is no derivation for Eq. (2.36) but it will turn out that this is indeed a reasonable choice. In particular we will show that in the limit of small  $\epsilon$  a rapid decay for the hybridization  $V_{k;}$  is obtained in this way. Thus, the part  $A_k^0(\epsilon; \epsilon)$  of the generator is not important anymore for the renormalization procedure and can be neglected in the following. In Eq. (2.36),  $\epsilon$  denotes an energy constant to ensure a dimensionless  $A_k^0(\epsilon; \epsilon)$ . Note that  $A_k^0(\epsilon; \epsilon)$  is chosen proportional to  $\epsilon$  to reduce the impact of the actual value of  $\epsilon$  on the final results of the renormalization.

In order to derive continuous renormalization equations note that the parameter  $A_k(\epsilon; \epsilon)$  is approximately proportional to  $\epsilon$ . By neglecting the part  $A_k^0(\epsilon; \epsilon)$  of the generator one can rewrite Eqs. (2.28) and (2.29) in the limit  $\epsilon \rightarrow 0$

$$\frac{d\epsilon_{k;}^\dagger}{d\epsilon} = -2V_{k;}\epsilon_{k;} \quad (2.37)$$

$$\frac{d\epsilon_{k;}}{d\epsilon} = +2V_{k;}\epsilon_{k;} \quad (2.38)$$

where higher order terms have been neglected. Furthermore, we define

$$\epsilon_{k;}(\epsilon) = \lim_{\epsilon \rightarrow 0} \frac{A_k^0(\epsilon; \epsilon)}{\epsilon}; \quad (2.39)$$

$$= \frac{\epsilon_{k;}^\dagger \epsilon_{k;} V_{k;}}{\epsilon_{k;}^\dagger \epsilon_{k;}}: \quad (2.40)$$

A similar equation can also be derived for  $V_{k;}$ ,

$$\frac{dV_{k;}}{d\epsilon} = (\epsilon_{k;}^\dagger \epsilon_{k;}) \epsilon_{k;}: \quad (2.40)$$

To solve these equations we rewrite (2.40),

$$\epsilon_{k;} = \frac{1}{\epsilon_{k;}^\dagger \epsilon_{k;}} \frac{dV_{k;}}{d\epsilon}; \quad (2.41)$$

and insert into (2.39). Using  $\epsilon_{k;}^\dagger + \epsilon_{k;} = \epsilon_{k;}^\dagger + \epsilon_{k;}$  we obtain

$$0 = \frac{d}{d\epsilon} (\epsilon_{k;}^\dagger)^2 (\epsilon_{k;}^\dagger + \epsilon_{k;}) \epsilon_{k;} + V_{k;}^2: \quad (2.42)$$

Eq. (2.42) is easily integrated and leads to a quadratic equation for  $\epsilon_{k;}^\dagger = \lim_{\epsilon \rightarrow 0} \epsilon_{k;}^\dagger$ , which corresponds to the former result (2.33). Moreover,  $\epsilon_{k;}^\dagger$  is found from  $\epsilon_{k;}^\dagger + \epsilon_{k;} = \epsilon_{k;}^\dagger + \epsilon_{k;}$ . According to (2.40) and (2.39) the  $\epsilon$ -dependence of  $V_{k;}$  is governed by

$$\frac{d \ln V_{k;}}{d\epsilon} = \frac{(\epsilon_{k;}^\dagger \epsilon_{k;})^2}{[\epsilon_{k;}^\dagger \epsilon_{k;}]^2} (\epsilon_{k;}^\dagger \epsilon_{k;}) \quad (2.43)$$

As one can easily see from Eq. (2.43),

- (i) the interaction  $V_{k;}$  is always renormalized to smaller values when the cut-off energy  $\epsilon$  is lowered,
- (ii) and at  $\epsilon = \epsilon_{k;}^\dagger \epsilon_{k;}$  the renormalized coupling  $V_{k;}$  vanishes, i.e. it has completely integrated out by the present choice of the generator  $P(\epsilon)X_{k;}$ .



### III. RENORMALIZATION OF THE ELECTRON-PHONON INTERACTION

The classical BCS-theory (26) is essentially based on attractive electron-electron interactions (27). It is well-known that such an interaction can be mediated via phonons coupled to the electronic system (28). In this section we want to revisit this problem because it has been studied (20; 29; 30) by Wegner's flow equation method (8), by a similarity transformation proposed by Glazek and Wilson (6; 7), and by the PRM (10). Therefore, the electron-phonon interaction is a perfectly suited test case to discuss differences and similarities of the three methods. In this section we consider the following Hamiltonian

$$H = \sum_{k; \sigma} \epsilon_k c_{k\sigma}^\dagger c_{k\sigma} + \sum_{q; \sigma} \hbar \omega_q b_{q\sigma}^\dagger b_{q\sigma} + \sum_{k, q; \sigma} g_{k, q; \sigma} b_{q\sigma}^\dagger c_{k+q, \sigma} + \sum_{k, q; \sigma} b_{q\sigma} c_{k+q, \sigma}^\dagger c_{k, \sigma} \quad (3.1)$$

which describes electrons  $c_{k\sigma}^\dagger$  and phonons  $b_{q\sigma}^\dagger$  that interact with each other.

In the following we apply a slightly modified version of the PRM to the electron-phonon problem (3.1) in order to derive an effective electron-electron interaction. It turns out that Fröhlich's transformation (28) is re-examined in this way.

In IIIB the approach is modified in the spirit of the ideas developed in subsections IIF and IIG. Thus, allowing a more continuous renormalization of the electron-phonon interaction we derive the result of Ref. 29 obtained by the flow equation method.

In subsection IIIC a much more sophisticated scheme is introduced by adding a symmetry breaking field to the Hamiltonian so that a gap equation can be derived. The effective electron-electron interaction is then obtained by comparing with the famous BCS-gap equation. The strategy to introduce symmetry breaking fields turns out to be of general importance for the investigation of phase transitions within the PRM.

Finally, the different results for the electron-phonon interaction (3.1) are discussed in subsection IIID.

#### A. Fröhlich's transformation

In this subsection we want to apply the PRM to the electron-phonon problem (3.1) in order to derive an effective electron-electron interaction. Here, we start from the renormalization ansatz,

$$H = H_0 + H_{1; \sigma} \quad (3.2)$$

$$H_0 = \sum_{k; \sigma} \epsilon_k c_{k\sigma}^\dagger c_{k\sigma} + \sum_{q; \sigma} \hbar \omega_q b_{q\sigma}^\dagger b_{q\sigma}$$

$$H_{1; \sigma} = \sum_{k, q; \sigma} g_{k, q; \sigma} b_{q\sigma}^\dagger c_{k+q, \sigma} + \sum_{k, q; \sigma} b_{q\sigma} c_{k+q, \sigma}^\dagger c_{k, \sigma}$$

$$H_{1; \sigma}^{\text{el;el}} = \sum_{k; \sigma, k'; \sigma'} V_{k, k'; \sigma, \sigma'} c_{k+q, \sigma}^\dagger c_{k, \sigma} c_{k', \sigma'}^\dagger c_{k', \sigma'}$$

that was also used in Ref. 29 where the flow equation method was applied to the same system. Note that the parameters of  $H_{1; \sigma}$  contain a cutoff function in order to ensure that only transitions with energies smaller than  $\hbar \omega_q$  are included. The parameters of  $H_{1; \sigma}^{\text{el;el}}$  depend on the energy cutoff because all transitions with energies larger than  $\hbar \omega_q$  have already been integrated out. However, we shall restrict ourselves to the second order renormalization contributions to  $H_{1; \sigma}$ . Therefore,  $H_0$  is assumed to be independent.

In the following we want to integrate out all transitions which create or annihilate phonons, however keeping all electronic transitions. Therefore, the present calculation differs from the previous ones where all parts of the 'unperturbed Hamiltonian'  $H_0$  were subject to the renormalization procedure. As it turns out, the electron-phonon coupling will be replaced by an effective electron-electron interaction. However, the final Hamiltonian containing the electron-electron interaction is not diagonal any more as required for the standard PRM. Instead, we want to derive a block-diagonal Hamiltonian so that the renormalization approach has to be modified. For this purpose, we define projection operators  $P^{\text{ph}}$  and  $Q^{\text{ph}}$  that are defined with respect to the phonon part of the unperturbed Hamiltonian  $H_0$ . These new projectors now replace those of the full unperturbed Hamiltonian.

Thus, from  $Q^{\text{ph}} H_{1; \sigma} = 0$  we conclude  $g_{k, q; \sigma} = \delta_{k, k+q} g_{k, q; \sigma}$ , where we have defined  $\delta_{k, k+q} = (\delta_{k, k+q})$ . Moreover, following Ref. 29, the generated electron-electron interaction  $H_{1; \sigma}^{\text{el;el}}$  is not considered in determining the generator of the unitary transformation (2.17). Thus, the generator can be written as

$$X_{1; \sigma} = \sum_{k, q; \sigma} A_{k, q; \sigma}(\hbar \omega_q) b_{q\sigma}^\dagger c_{k+q, \sigma} + \sum_{k, q; \sigma} b_{q\sigma} c_{k+q, \sigma}^\dagger c_{k, \sigma} \quad (3.3)$$

where the parameter  $A_{k, q; \sigma}(\hbar \omega_q)$  needs to be properly determined in the following: Corresponding to (2.18),

$$Q^{\text{ph}}(\hbar \omega_q) H(\hbar \omega_q) = 0 \quad (3.4)$$

must be fulfilled.

As already discussed, the part  $P^{\text{ph}}(\hbar \omega_q) X_{1; \sigma}$  of the generator (3.3) of the unitary transformation is not fixed by the PRM. Thus, the parameters  $A_{k, q; \sigma}(\hbar \omega_q)$  have the

following general form

$$A_{k;q}(\epsilon) = A_{k;q}^0(\epsilon) \delta_{k,q} [1 - \delta_{k,q}] + A_{k;q}^{\text{ph}}(\epsilon) \delta_{k,q} \delta_{k,q} : (3.5)$$

Note that both parts of  $A_{k;q}(\epsilon)$  include the factor  $\delta_{k,q}$ . However, in the following  $P(\epsilon)X$  and  $A_{k;q}^0(\epsilon)$  are set to zero for simplicity. Note that a different choice for  $A_{k;q}^0(\epsilon)$  will be used in the subsequent subsection.

We restrict ourselves to second order renormalization contributions so that the unitary transformation (2.17) can easily be evaluated where operator terms are only kept if they are included in the ansatz (3.2). Thus, we directly obtain difference equation for the electron-phonon coupling,

$$g_{k;q} = g_{k;q} + \epsilon_q [A_{k+q;q}(\epsilon) - A_{k;q}(\epsilon)] : (3.6)$$

and for the effective electron-electron interaction,

$$\begin{aligned} V_{k,jk^0;q} &= V_{k,jk^0;q} + \epsilon_q A_{k^0;q}(\epsilon) g_{k+q;q} \\ &= A_{k^0;q}(\epsilon) g_{k;q} \\ &+ \frac{1}{2} (\epsilon_{k+q} - \epsilon_k - \epsilon_q) A_{k^0;q}(\epsilon) A_{k;q}(\epsilon) \\ &+ \frac{1}{2} (\epsilon_{k+q} - \epsilon_k + \epsilon_q) A_{k+q;q}(\epsilon) A_{k^0;q}(\epsilon) : \end{aligned} \quad (3.7)$$

Because we have set  $P(\epsilon)X = 0$ , renormalization contributions only appear if the phonon energy  $\epsilon_q$  is in the energy shell between  $(\epsilon_k)$  and  $(\epsilon_{k+q})$ . Consequently, we find a step-like renormalization of the electron-phonon coupling  $g_{k;q}$  and the generated electron-electron interaction  $V_{k,jk^0;q}$ . The parameter  $A_{k;q}(\epsilon)$  defined in (3.5) has to be chosen in such a way that  $g_{k;q} = g_{k;q}$ . From equation (3.6) we obtain

$$A_{k;q}(\epsilon) = \frac{g_q}{\epsilon_k - \epsilon_{k+q} - \epsilon_q} \delta_{k,q} [1 - \delta_{k,q}] : (3.8)$$

As one can see by inserting Eq. (3.8) into (3.6), the electron-phonon coupling has no  $k$ -dependence in the present approximation, i.e.  $g_{k;q} = g_q$ .

Now we insert Eq. (3.8) into the renormalization equation (3.7) and consider the limit  $\epsilon \rightarrow 0$ ,

$$V_{k,jk^0;q} = \lim_{\epsilon \rightarrow 0} V_{k,jk^0;q} = \frac{\epsilon_q g_q^2}{(\epsilon_{k+q} - \epsilon_k)^2 - \epsilon_q^2} ; \quad (3.9)$$

where we exactly find Frohlich's result (28).

## B. Continuous transformation

Wegner's flow equation method (8) was applied to the electron-phonon system (3.1) in Ref. 29 where a renormalization ansatz similar to (3.2) was used. However, a

less singular expression for the effective electron-electron interaction could be derived in this way. In the following we want to analyze how this different result can be understood in the framework of the PRM.

In order to derive continuous renormalization equations the part  $P^{\text{ph}}(\epsilon)X$  of the generator of the unitary transformation is chosen to be non-zero so that now  $A_{k;q}^0(\epsilon)$  needs to be considered in Eq. (3.5). Furthermore,  $A_{k;q}^0(\epsilon)$  can be neglected if  $A_{k;q}^0(\epsilon)$  leads to a rapid decay of the interaction terms. Thus, neglecting  $A_{k;q}^0(\epsilon)$  and employing the limit  $\epsilon \rightarrow 0$  we obtain from Eqs. (3.6) and (3.7)

$$\frac{d}{d\epsilon} g_{k;q} = [\epsilon_{k+q} - \epsilon_k - \epsilon_q] g_{k;q} ; \quad (3.10)$$

$$\begin{aligned} \frac{d}{d\epsilon} V_{k,jk^0;q} &= g_{k+q;q} \epsilon_{k^0;q} \\ &+ g_{k;q} \epsilon_{k^0+q;q} : \end{aligned} \quad (3.11)$$

Here, we introduced  $g_{k;q} = \lim_{\epsilon \rightarrow 0} A_{k;q}^0(\epsilon) = g_{k;q}$ . Again the parameter  $A_{k;q}^0(\epsilon)$  is chosen proportional to  $\epsilon$  so that the third and the fourth term on the right side of Eq. (3.7) can be neglected in the limit  $\epsilon \rightarrow 0$ .

The commonly used generator of the flow equation method is chosen in such a way that the matrix elements of the interaction, which shall be integrated out, show an exponential decay with respect to the flow parameter. Consequently, all matrix elements change continuously during the renormalization procedure. We adapt the idea of such a continuous renormalization and assume an exponential decay for the electron-phonon interaction,

$$g_{k;q} = g_q \exp \left( - \frac{(\epsilon_{k+q} - \epsilon_k - \epsilon_q)^2}{(\epsilon_q)^2} \right) \delta_{k,q} ; \quad (3.12)$$

where  $\epsilon$  is just a constant to ensure a dimensionless exponent. Note that ansatz (3.12) is inspired by the results of Ref. 29. Of course, Eq. (3.12) is only useful as long as the considered renormalization contributions are restricted to second order in the original electron-phonon interaction. Note also that ansatz (3.12) meets the basic requirement (2.18) of the PRM,  $Q(\epsilon)H(\epsilon) = 0$ .

Now we need to determine the parameter  $g_{k;q}$  of the unitary transformation. For this purpose, Eq. (3.10) is divided by  $g_{k;q}$  and integrated between the cutoff  $\epsilon_q$  and 1 by using Eq. (3.12). We find

$$g_{k;q} = \frac{g_q [\epsilon_{k+q} - \epsilon_k - \epsilon_q]}{(\epsilon_q)^2} ; \quad (3.13)$$

Note that this result is equivalent to the choice for  $A_{k;q}^0(\epsilon)$  used for the Fano-Anderson model in IIG [compare with equations (2.36) and (2.39)].

Using this solution and the ansatz (3.12) for the electron-phonon coupling  $g_{k;q}$ , Eq. (3.11) is easily integrated where the constant  $\epsilon$  is canceled. Thus, the

renormalized values  $V_{k;k^0;q} = \lim_{\lambda \rightarrow 0} \lambda V_{k;k^0;q}$ , can be obtained and reads

$$V_{k;k^0;q} = \frac{g_q^2 \left( \epsilon_{k^0+q} \epsilon_{k^0} \epsilon_q \right)}{\left( \epsilon_{k+q} \epsilon_{k^0+q} \right)^2 + \left( \epsilon_{k^0+q} \epsilon_{k^0} \epsilon_q \right)^2} \cdot \frac{g_q^2 \left( \epsilon_{k^0+q} \epsilon_{k^0} \epsilon_q \right)}{\left( \epsilon_{k+q} \epsilon_{k^0+q} \right)^2 + \left( \epsilon_{k^0+q} \epsilon_{k^0} \epsilon_q \right)^2} : \quad (3.14)$$

This is the final version of the effective electron-electron interaction after eliminating the electron-phonon interaction. Obviously, (3.14) differs from Frohlich's result (28) that had been derived above (3.9). However, Eq. (3.14) coincides with the result of Ref. 29 that had been obtained by Wegner's flow equation method (8).

At this point it is important to notice that the approaches of IIIA and IIIB are based on the same renormalization ansatz (3.2). Therefore, the different results are only caused by different choices for the generator. Due to the continuous renormalization, the electron-phonon coupling becomes dependent on the electronic one-particle energies  $\epsilon_k$  so that the approach of IIIB involves more degrees of freedom.

The main goal of this subsection was to demonstrate that Wegner's flow equation method (8) can be understood within the PRM (10), as already for the case of the Fano-Anderson model in the previous section. However, the idea of a continuous renormalization, as implemented here, can also be very useful for other applications. In this regards, the discussion line needs to be changed: One starts from an ansatz for the generator  $X$ ; of the unitary transformation similar to Eqs. (3.3), (3.13), and demonstrates afterwards that the interaction decays as function of  $\lambda$  as required.

#### C. Improved renormalization scheme and BCS-gap equation

So far the discussion of the electron-phonon problem was focused on the phonon-induced electron-electron interaction. Thus, we derived block-diagonal Hamiltonians with constant phonon occupation numbers within each block. However, in the following we want to tackle the electron-phonon problem (3.1) in a different way because an effective phonon mediated electron-electron interaction is mainly discussed with respect to superconductivity. The idea is to obtain the superconducting properties directly from the electron-phonon system.

The goal is again to decouple the electron and the phonon system but now we want to derive a truly diagonal renormalized Hamiltonian. For this purpose the PRM shall be applied to the electron-phonon system (3.1) in conjunction with a Bogoliubov transformation (31) as it was done in Ref. 20.

Whereas the Hamiltonian (3.1) is gauge invariant, a BCS-like Hamiltonian breaks this symmetry (26). Therefore, in order to describe superconducting properties, the

renormalized Hamiltonian should contain a symmetry breaking field as well so that the renormalization ansatz reads

$$\begin{aligned} H &= H_0 + H_1; \\ H_0 &= \sum_k \epsilon_k c_k^\dagger c_k + \sum_q \epsilon_q b_q^\dagger b_q \\ &\quad + \sum_k \left( C_k c_k^\dagger c_{k\#} + C_k c_{k\#} c_k \right) + C; \\ H_1 &= P \sum_{k,q} g_q c_k^\dagger c_{k+q} b_q^\dagger + c_{k+q}^\dagger c_k b_q : \end{aligned} \quad (3.15)$$

Here, the 'fields'  $c_k$  and  $b_k$  break the gauge invariance and can be interpreted as the superconducting gap function. The initial values for  $C_k$  and the energy shift  $C$  are given by those of the original model,  $C_k = 0$ ,  $C = 0$ . Note that in the following the projectors  $P$  and  $Q$  are defined as usual with respect to  $H_0$ , and not only to the phonon part. Furthermore, renormalization contributions to electronic and phononic one-particle energies and to the electron-phonon coupling will be neglected for simplicity.

At this point it is important to realize that the introduction of symmetry breaking fields is a general concept to study phase transitions within the PRM. The same approach has also been successfully applied to the Holstein model and its quantum phase transition (32; 33); this model will be discussed in Sec. VI.

To perform our renormalization scheme as introduced in section II we need to solve the eigenvalue problem of  $H_0$ . For this purpose we utilize the well-known Bogoliubov transformation (31) and introduce new dependent fermionic operators,

$$\begin{aligned} \gamma_k &= u_k c_k + v_k c_{k\#}; \\ \gamma_{k\#} &= u_k c_{k\#} + v_k c_k; \end{aligned} \quad (3.16)$$

where the coefficients read

$$\begin{aligned} u_k &= \frac{1}{2} \left( 1 + \sqrt{1 + \frac{\epsilon_k^2}{\epsilon_k^2 + j_{k\#}^2}} \right); \\ v_k &= \frac{1}{2} \left( 1 - \sqrt{1 + \frac{\epsilon_k^2}{\epsilon_k^2 + j_{k\#}^2}} \right); \end{aligned} \quad (3.17)$$

Hence,  $H_0$  can be rewritten in diagonal form,

$$\begin{aligned} H_0 &= \sum_k E_k \gamma_k^\dagger \gamma_k + \sum_q \epsilon_q b_q^\dagger b_q + C \\ &\quad + \sum_k \left( \epsilon_k \gamma_k^\dagger \gamma_{k\#} + \epsilon_k \gamma_{k\#}^\dagger \gamma_k \right) \end{aligned} \quad (3.18)$$

where the fermionic excitation energies are given by  $E_k = \sqrt{\epsilon_k^2 + j_{k\#}^2}$ .

In the following, we restrict ourselves to second order renormalization contributions so that the first order of the generator  $X$ ; of the unitary transformation is sufficient [see Eq. (2.12) and the discussion in II.B]. Thus,  $X$ ; can be written as (2.17),

$$X = \sum_i \left[ A_{k;q}(\epsilon) b_{q,k}^y c_{k+q}^\dagger - b_{q,k+q}^y c_k \right] \quad (3.19)$$

where

$$A_{k;q}(\epsilon) = \frac{g_q}{\epsilon_k - \epsilon_{k+q} - \epsilon_q} A_{k;q}(\epsilon); \quad (3.20)$$

$$A_{k;q}(\epsilon) = \left[ \epsilon_k - \epsilon_{k+q} - \epsilon_q \right]^{-1} \left[ \epsilon_k - \epsilon_{k+q} - \epsilon_q \right];$$

Note that the generator  $X$ ; as defined in Eq. (3.19) almost completely agrees with the one used to re-examine Fröhlich's transformation in subsection III.A [see Eqs. (3.3) and (3.8)]. However, now the functions do not only refer to the phonon energies  $\epsilon_q$  but also to the electronic one-particle energies  $\epsilon_k$  because of the different definitions of the  $P$  projection operators.

To perform the renormalization step reducing the cut-off from  $\epsilon_F$  to  $\epsilon_c$ , one would need to express the electron creation and annihilation operators by the quasiparticle operators (3.16). After considering the renormalization contributions, the quasiparticle operators have to be transformed back to the original electron operators. However, this involved procedure is only necessary if we are interested in renormalization contributions beyond second order perturbation theory. Therefore, here the symmetry breaking fields  $\epsilon_k$  and  $\epsilon_{k+q}$  are only generated by the renormalization scheme but not considered in the evaluation of energy denominators or projection operators.

Taking into account all simplifications related with second order perturbation theory, the unitary transformation (2.17) is easily evaluated where generated operator terms are only kept if their mean-field approximations renormalize the symmetry breaking fields,  $\epsilon_k$  and  $\epsilon_{k+q}$ , or the energy shift,  $C$ . Thus, for sufficiently small steps we obtain the following renormalization equations

$$\epsilon_k; = \epsilon_k; + 2 \sum_q \frac{g_q^2}{\epsilon_k - \epsilon_{k+q} - \epsilon_q} \epsilon_k \epsilon_{k+q} \quad (3.21)$$

$$C(\epsilon) = C + \sum_k \frac{g_k^2}{\epsilon_k - \epsilon_{k+q} - \epsilon_q} C_{k;q} C_{k+q}; \quad (3.22)$$

By summing up all difference equations between the cut-off of the original model and the lower cut-off  $\epsilon_c$ , one easily finds

$$\tilde{\epsilon}_k = \epsilon_k + 2 \sum_q \frac{g_q^2}{\epsilon_k - \epsilon_{k+q} - \epsilon_q} \epsilon_k \epsilon_{k+q} \quad (3.23)$$

$$\tilde{C} = C + \sum_k \frac{g_k^2}{\epsilon_k - \epsilon_{k+q} - \epsilon_q} \tilde{\epsilon}_k \epsilon_{k+q}; \quad (3.24)$$

Here we defined  $\tilde{\epsilon}_k = \lim_{\epsilon_c \rightarrow 0} \epsilon_k$ ; ,  $\tilde{C} = \lim_{\epsilon_c \rightarrow 0} C$ .

The final Hamiltonian  $\tilde{H} = \lim_{\epsilon_c \rightarrow 0} H$  can easily be diagonalized by a Bogoliubov transformation and reads according (3.18)

$$\tilde{H} = \sum_k \tilde{E}_k \tilde{c}_k^\dagger \tilde{c}_k + \sum_k \tilde{E}_k \tilde{c}_k^\dagger \tilde{c}_k + \sum_q \epsilon_q b_q^\dagger b_q + C \quad (3.25)$$

where  $\tilde{E}_k = \lim_{\epsilon_c \rightarrow 0} E_k$ ; ,  $\tilde{\epsilon}_k = \lim_{\epsilon_c \rightarrow 0} \epsilon_k$ ; , and  $\tilde{\epsilon}_k = \lim_{\epsilon_c \rightarrow 0} \epsilon_k$ ; . Its parameters depend on the original system (3.1), on the initial conditions,  $\epsilon_k; = 0, C = 0$ , and on expectation values  $c_{k;}, c_{k+q};$  that need to be determined self-consistently. Following the approach of Ref. 20, we consider the free energy which can be calculated either from  $H$  or from the renormalized Hamiltonian  $\tilde{H}$ . Thus, the required expectation values are easily found by functional derivatives,  $c_{k;}, c_{k+q}; = \frac{\partial F}{\partial \epsilon_{k;}}$ , so that Eq. (3.23) can be rewritten as

$$\tilde{\epsilon}_k = \sum_q \left( \frac{2 g_q^2}{\epsilon_k - \epsilon_{k+q} - \epsilon_q} \epsilon_k \epsilon_{k+q} \right) \quad (3.26)$$

where the initial condition  $\epsilon_k; = 0$  has been used. Eq. (3.26) has the form of the famous BCS-gap equation so that the term inside the braces  $\epsilon_k \epsilon_{k+q}$  can be interpreted as parameter of the effective phonon induced electron-electron interaction,

$$V_{k;q} = \frac{g_q^2}{\epsilon_k - \epsilon_{k+q} - \epsilon_q} \quad (3.27)$$

which is responsible for the formation of Cooper pairs. Even though we have here derived an effective electron-electron interaction as well there is a significant difference to the approaches of III.A and III.B: In the present formalism both the attractive electron-electron interaction and the superconducting gap function were derived in one step by applying the PRM to the electron-phonon system (3.1) with additional symmetry breaking fields.

## D. Discussion

In the following we want to discuss the different approaches to the phonon-induced effective electron-electron interaction in more detail. At first we summarize the results derived above where we focus on the interaction between electrons of a Cooper pair. Fröhlich's classical result [see Ref. 28 and Eq. (3.9)] reads

$$V_{k; k+q}^{\text{Fröhlich}} = \frac{\hbar^2 \omega_q^2}{(\epsilon_{k+q} - \epsilon_k)^2 + \omega_q^2}; \quad (3.28)$$

However, there is an important problem related with Eq. (3.28): It diverges at  $\hbar^2 \omega_q^2 = (\epsilon_{k+q} - \epsilon_k)^2$ . Thus, a cutoff function is introduced by hand in the classical BCS-theory to suppress repulsive contributions to the effective electron-electron interaction.

In contrast to the Fröhlich interaction (3.28), the results obtained by Wegner's flow equation method (29), by similarity transformation (30), and by the PRM (20) are less singular,

$$V_{k; k+q}^{\text{Lenz/Wegner}} = \frac{\hbar^2 \omega_q^2}{(\epsilon_{k+q} - \epsilon_k)^2 + \omega_q^2}; \quad (3.29)$$

$$V_{k; k+q}^{\text{Mielke}} = \frac{\hbar^2 \omega_q^2 (\epsilon_{k+q} - \epsilon_k + \omega_q)}{\epsilon_{k+q}^2 - \epsilon_k^2 + \omega_q^2}; \quad (3.30)$$

$$V_{k; k+q}^{\text{Hübisch/Becker}} = \frac{\hbar^2 \omega_q^2 (\epsilon_q - \epsilon_{k+q} - \epsilon_k)}{\epsilon_{k+q}^2 - \epsilon_k^2 + \omega_q^2}; \quad (3.31)$$

(Note that Eqs. (3.29) and (3.31) have already been derived above, compare with (3.14) and (3.27). The dependence of the electronic and phononic one-particle energies are suppressed in (3.30) for simplicity.) All three results for the effective phonon-mediated electron-electron interaction are never repulsive as long as  $\omega_q > 0$  is fulfilled.

At first we want to discuss Mielke's result (30), an effective electron-electron interaction (3.30) that depends on the energy cutoff. As Wegner's flow equation method (8), the used similarity transformation (6; 7) is based on continuous unitary transformations and leads to differential equations for the parameters of the Hamiltonian. However, like the PRM, the similarity transformation leads to a band-diagonal structure of the renormalized Hamiltonian with respect to the eigenenergies of the unperturbed Hamiltonian whereas the flow equation method generates block-diagonal Hamiltonians.

Mielke derived the phonon-mediated electron-electron interaction (3.30) by eliminating excitations with energies larger than  $\omega$  where excitation energies are measured with respect to the unperturbed Hamiltonian consisting of both electronic and bosonic degrees of freedom. The obtained effective interaction becomes independent for the Einstein model (of dispersion-less phonons) if  $\omega$  is

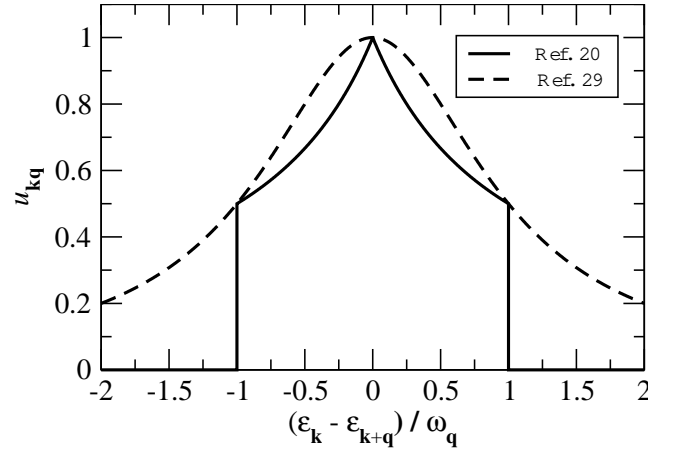


FIG. 1 Comparison of the effective electron-electron interaction obtained by the PRM (full line) and by Wegner's flow equations (dashed line). Here, the dimensionless quantity  $u_{k,q} = \frac{\omega_q V_{k,q}}{\hbar^2 \omega_q^2}$  has been introduced.

chosen smaller than the phonon frequency  $\omega_0$ . For this case Mielke's result (3.30) is very similar to ours (3.31) obtained by the PRM with symmetry-breaking fields. However, in contrast to our result (3.31), the cutoff function  $(\omega_q - \epsilon_{k+q} - \epsilon_k)$  is absent in (3.30). This difference might be related with different choices for the generator of the unitary transformation in the two methods but could also be caused by a systematic problem in Mielke's approach: Setting  $\omega = 0$ , the renormalized Hamiltonian contains non-diagonal terms with respect to the used unperturbed Hamiltonian. This seems to contradict a basic premise of the similarity transformation.

Lenz and Wegner (29) applied the flow equation method to the electron-phonon problem as discussed here and obtained an effective electron-electron interaction as shown in Eq. (3.29). As one can see in Fig. 1, their result is quite similar to ours (3.31) derived using the PRM as long as  $\omega_q - \epsilon_{k+q} - \epsilon_k$  is fulfilled. However, in contrast to our result (3.31), the interaction (3.29) remains finite even for  $\omega_q < \epsilon_{k+q} - \epsilon_k$ . Probably, this difference is caused by the different choices for the generator of the unitary transformation that also require different approximations in order to obtain closed sets of renormalization equations.

## IV. HEAVY-FERMION BEHAVIOR IN THE PERIODIC ANDERSON MODEL

The periodic Anderson model (PAM) is considered to be the basic microscopic model for the theoretical investigation of heavy-fermion (HF) systems (34). It describes localized, strongly correlated  $f$  electrons interacting with itinerant conduction electrons. Here we focus on the limit of infinitely large Coulomb repulsion on  $f$  sites so that

the Hamiltonian of the PAM can be written as

$$H = H_0 + H_1; \quad (4.1)$$

$$H_0 = \sum_{i,m} \epsilon_f \hat{f}_{im}^\dagger \hat{f}_{im} + \sum_{k,m} \epsilon_k \hat{c}_{km}^\dagger \hat{c}_{km};$$

$$H_1 = \frac{1}{N} \sum_{k,i,m} V_k \hat{f}_{im}^\dagger \hat{c}_{km} e^{ikR_i} + \text{h.c.} :$$

The one-particle energies  $\epsilon_f$  and  $\epsilon_k$ , and, as a simplification, both types of electrons have the same angular momentum index  $m = 1 ::: f$ . The Hubbard operators,

$$\hat{f}_{im}^\dagger = \hat{f}_{im}^\dagger \sum_{m' \in m} (1 - \hat{f}_{im'}^\dagger \hat{f}_{im'});$$

take into account the infinitely large local Coulomb repulsion and only allow either empty or singly occupied  $f$  sites.

The PRM has already been applied to the PAM in Ref. 21; 22 where approximations have been employed that allow to map the renormalization equations of the PAM onto those of the uncorrelated Fano-Anderson model (see subsection II E). Thus, HF behavior and a possible valence transition between mixed and integral valent states could be studied. However, the approach of Refs. 21; 22 has a significant disadvantage: the renormalization of the one-particle energies show as function the cutoff a steplike behavior that leads to serious problems in the (numerical) evaluation. Therefore, a constant renormalized  $f$  energy had to be chosen for all values of the energy cutoff to ensure a continuous behavior of the one-particle energies as required for physical reasons.

In the following we modify the approach of Refs. 21; 22 to ensure a more continuous renormalization of all parameters of the Hamiltonian. For this purpose, the ideas of II G and III B are transferred to the PAM. However, to explore all features of this continuous approach is beyond the scope of this review, we re-derive the analytical solution of Ref. 21 instead.

#### A. Renormalization ansatz

Much of the physics of the PAM (4.1) can be understood in terms of an effective uncorrelated model that consists of two non-interacting fermionic quasiparticle bands. Various theoretical approaches have been used to generate such effective Hamiltonians; the most popular among them is the slave-boson mean-field (SB) theory (11; 12). However, as discussed in Ref. 22, such approaches do not prevent from unphysical multiple occupation of  $f$  sites and are therefore restricted to heavy-fermion like solutions. [The SB solutions break down if the original  $f$  level  $\epsilon_f$  is located too far below the Fermi level or if the hybridization between  $f$  and conduction electrons becomes too weak (35).]

To reliably prevent the system from unphysical states with multiple occupations of  $f$  sites we here follow Ref. 22 and start from a renormalization ansatz that keeps the Hubbard operators during the whole renormalization procedure,

$$H = H_0; + H_1; ; \quad (4.2)$$

$$H_0; = e_f; \sum_{k,m} \hat{f}_{km}^\dagger \hat{f}_{km} + \sum_{k,m} \epsilon_k; \hat{c}_{km}^\dagger \hat{c}_{km} + E; ;$$

$$H_1; = P H_1; = \sum_{k,m} V_k; \hat{f}_{km}^\dagger \hat{c}_{km} + \text{h.c.} :$$

Eq. (4.2) is obtained after all excitations between eigenstates of  $H_0;$  with transition energies larger than the cutoff have been eliminated, i.e.  $Q H = 0$  holds. Furthermore, we introduced Fourier transformed Hubbard operators,

$$\hat{f}_{km}^\dagger = \frac{1}{N} \sum_i \hat{f}_{im}^\dagger e^{ikR_i};$$

The dependencies of the parameters are caused by the renormalization procedure. Note that  $V_k;$  includes a cutoff function in order to ensure that the requirement  $Q H = 0$  is fulfilled. Furthermore, an additional energy shift  $E$  and direct hopping between  $f$  sites,

$$\hat{f}_{km}^\dagger \hat{f}_{km} = \frac{1}{N} \sum_{i,j \in i} \hat{f}_{im}^\dagger \hat{f}_{jm} e^{ik(R_i - R_j)};$$

have been generated. Finally, we need the initial parameter values of the original model (with cutoff) to fully determine the renormalization,

$$e_f; = \epsilon_f; \quad \epsilon_k; = 0; \quad \epsilon_k; = \epsilon_k; \quad E = 0; \quad (4.3)$$

$$V_k; = V_k;$$

To implement our PRM scheme we also need the commutator of the unperturbed part  $H_0;$  of the dependent Hamiltonian  $H$  with the interaction  $H_1;$  (in the present case the hybridization between  $f$  and conduction electrons). To shorten the notation we here introduce the (unperturbed) Liouville operator  $L_0;$  that is defined as  $L_0; A = [H_0; ; A]$  for any operator  $A$ . Because of the correlations included in the Hubbard operators  $\hat{f}_{km}^\dagger$ , the required commutator relation can not be calculated exactly and additional approximations are necessary. Here, the one-particle operators  $\hat{f}_{km}^\dagger$  and  $\hat{c}_{km}^\dagger$  are considered as approximative eigenoperators of  $L_0;$  so that we obtain

$$L_0; \hat{f}_{km}^\dagger \hat{c}_{km} = (\epsilon_f; + D_k; \quad \epsilon_k;) \hat{f}_{km}^\dagger \hat{c}_{km}; \quad (4.4)$$

Here we introduced the local  $f$  energy,

$$\epsilon_f; = e_f; - D; \quad (4.5)$$



evaluation of the free energy is complicated as long as the renormalized Hamiltonian contains Hubbard operators  $\hat{f}_{km}$ . Thus, here it would be more convenient to use the second strategy to calculate expectation values and to derive renormalization equations for additional operator expressions (see Refs. 21 and 22 for more details). However, such involved approach is only needed in case of a numerical treatment of the renormalization equations which will be discussed below.

The further calculations can be simplified by considering the limit  $\beta \rightarrow 0$  and to transform the difference equations (4.7) – (4.11) into differential equations. For this purpose we define

$$\chi_k(\beta) = \lim_{\beta \rightarrow 0} \frac{A_k^{(0)}(\beta)}{\beta} \quad (4.12)$$

so that we obtain

$$\frac{d\chi_k}{d\beta} = 2D_k(\beta)V_k; \quad (4.13)$$

$$\frac{d\chi_k}{d\beta} = \frac{1}{D} \frac{d\chi_k}{d\beta} \quad (4.14)$$

$$\frac{d\epsilon_f}{d\beta} = \frac{1}{D} \frac{1}{N} \sum_k \left[ 1 + (\epsilon_f - 1) \sum_{km} c_{km}^y c_{km} \right] \frac{d\chi_k}{d\beta};$$

$$\frac{d\chi_k}{d\beta} = \frac{1}{N} \sum_{km} \left[ \chi_k(\beta) \chi_{km}(\beta) + \chi_k(\beta) \chi_{km}(\beta) \right] \quad (4.15)$$

$$\frac{dV_k}{d\beta} = \epsilon_f + D_k \chi_k; \quad (4.16)$$

$$\frac{dE}{d\beta} = N \sum_i \frac{d\epsilon_i}{d\beta} + \frac{1}{D} \sum_k \frac{d\chi_k}{d\beta}; \quad (4.17)$$

#### D. Analytical solution

In the following, we concentrate on an analytical solution of the renormalization equations (4.13)–(4.17) by assuming a independent energy of the  $f$  electrons. The aim is to demonstrate that the analytical solution of Ref. 21 can also be derived from the renormalization equations (4.13)–(4.17) or likewise (4.7)–(4.11) obtained here. In particular, we want to derive an analytical solution that describes HF behavior. As in Ref. 21, we use the following approximations:

- (i) All expectation values (which appear due to the employed factorization approximation) are considered as independent from the renormalization parameter  $\beta$  and are calculated with respect to the full Hamiltonian  $H$ .
- (ii) As mentioned, the dependence of the renormalized  $f$  level is neglected and we approximate  $\epsilon_f = D \chi_f$  to decouple the renormalization

of the different  $k$  values. Note that such a renormalized  $f$  energy is also used from the very beginning in the SB theory.

- (iii) To obtain the analytical solution of Ref. 21 we set  $\frac{1}{N} \sum_k \chi_k = 0$  for further simplification.

- (iv) The Hubbard operators are replaced by usual fermionic operators where we employ

$$\sum_k \hat{f}_{km}^y \hat{f}_{km} = \sum_k f_{km}^y f_{km} \quad \text{and}$$

$$\hat{f}_{km}^y \hat{f}_{km} = D f_{km}^y f_{km} : \quad (4.18)$$

Thus, on a mean-field level, the system is prevented from generating unphysical states but a multiple occupation of  $f$  sites is not completely suppressed by this approximation. Therefore, we can only obtain useful results as long as only very few  $f$  type states below the Fermi level are occupied.

It turns out that the analytical solution of Ref. 21 is obtained if the approximations (i)–(iii) are applied to the renormalization equations (4.13)–(4.17).

Employing approximation (iv), the desired renormalized Hamiltonian  $H^* = \lim_{\beta \rightarrow 0} H$  is a free system consisting of two non-interacting fermionic quasi-particle bands,

$$H^* = \sum_{km} \epsilon_k c_{km}^y c_{km} \quad (4.18)$$

$$+ \sum_{km} \epsilon_f + D \chi_k f_{km}^y f_{km} + E^* :$$

Eqs. (4.14) and (4.11) can be easily integrated between  $\beta = 0$  and the cutoff  $\beta$  of the original model,

$$\chi_k = \frac{1}{D} [\epsilon_k - \epsilon_f]; \quad (4.19)$$

$$E^* = N \sum_i \epsilon_i [\epsilon_f - \epsilon_f] + \frac{D}{D} \sum_k \epsilon_k [\epsilon_k - \epsilon_f] \quad (4.20)$$

where approximation (iii) has been used. The equation (4.13) can also be solved if the renormalizations of the different  $k$  values are decoupled from each other by approximations (i) and (ii). Thus, Eq. (4.16) can be rewritten as

$$\chi_k(\beta) = \frac{1}{\epsilon_f + \epsilon_k - 2\chi_k} \frac{dV_k}{d\beta}$$

and inserted into (4.13) so that we obtain

$$0 = \frac{d}{d\beta} \epsilon_k^2; \quad (\epsilon_f + \epsilon_k) \epsilon_k + D V_k^2; \quad (4.21)$$

Eq. (4.21) can easily be integrated and a quadratic equation for  $\epsilon_k = \lim_{\beta \rightarrow 0} \epsilon_k$  is obtained. Our recent work on the PAM (21; 22) has shown that the quasi-particles



in the renormalized Hamiltonian  $\tilde{H}$  (4.18) do not change their (c or f) character as function of the wave vector  $k$ . Therefore,  $u_k$  jumps between the two solutions of the obtained quadratic equation in order to minimize its deviations from the original  $u_k$ ,

$$u_k = \frac{u_f + u_k}{2} + \frac{\text{sgn}(u_f - u_k)}{2} W_k; \quad (4.22)$$

$$W_k = \frac{(u_k - u_f)^2 + 4D J_k^2}{2}; \quad (4.23)$$

The second quasi-particle band is given by

$$\epsilon_k = u_f + D \tilde{\epsilon}_k = \frac{u_f + u_k}{2} + \frac{\text{sgn}(u_f - u_k)}{2} W_k; \quad (4.24)$$

Thus, we have obtained the same effective Hamiltonian (4.18) and the same quasi-particle energies (4.22) and (4.24) as found in Ref. 21.

Finally, we need to determine the renormalized f energy  $u_f$  and the expectation values. Because the renormalized Hamiltonian (4.18) consists of non-interacting fermionic quasi-particles, it is straightforward to calculate all desired quantities from the free energy as it was done in Ref. 21. Because the effective model  $\tilde{H}$  is connected with the original Hamiltonian  $H$  by a unitary transformation the free energy can also be calculated from  $\tilde{H}$ ,

$$F = -\frac{1}{\beta} \ln \text{Tr} e^{-\beta \tilde{H}};$$

The expectation value of the f occupation is found from the free energy by functional derivative,

$$\langle n_i^f \rangle = \frac{1}{N} \frac{\partial F}{\partial u_f} = \frac{1}{N} \frac{\partial \tilde{H}}{\partial u_f}; \quad (4.25)$$

Thus, we finally obtain a relation of the following structure

$$0 = f::g \frac{\partial u_f}{\partial u_f} + f::g \frac{\partial \langle n_i^f \rangle}{\partial u_f}; \quad (4.26)$$

In the cases of fixed valence and heavy Fermion behavior the derivatives in Eq. (4.26) are non-zero so that both brace expressions can be set equal to zero to find equations of self-consistency for the renormalized f level and the averaged f occupation number,

$$\langle n_i^f \rangle = \frac{f}{N} \sum_k \left( f(u_k) \frac{1}{2} + \text{sgn}(u_f - u_k) \frac{u_k - u_f}{2W_k} \right) \quad (4.27)$$

$$+ \frac{f}{N} \sum_k \left( f(\epsilon_k) \frac{1}{2} + \text{sgn}(u_k - u_f) \frac{u_k - u_f}{2W_k} \right);$$

$$u_f - u_f = \frac{f}{N} \sum_k \text{sgn}(u_f - u_k) f(u_k) \frac{J_k J}{W_k} \quad (4.28)$$

$$+ \frac{f}{N} \sum_k \text{sgn}(u_k - u_f) f(\epsilon_k) \frac{J_k J}{W_k};$$

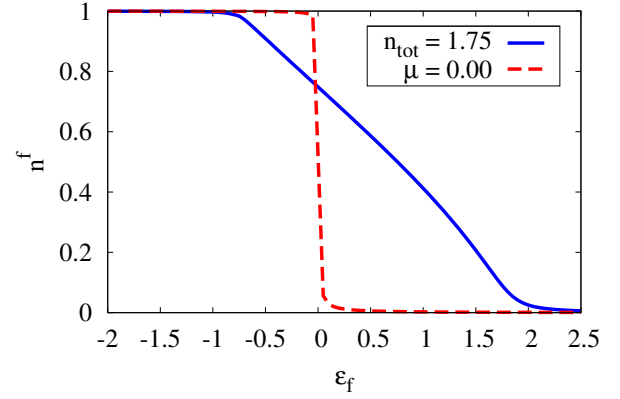


FIG. 2 (Color online) f-electron occupation number  $n^f_i = \langle n_i^f \rangle$  as function of the bare energy  $u_f$  for an one-dimensional lattice with 10000 sites for two cases: i) the total particle occupation  $n_{\text{tot}} = n^f + n^c = 1.75$  is fixed (in red) and (ii) the chemical potential (in green) is fixed. Moreover,  $u_f = 2$ ,  $V = 0.10(4t)$  and the temperature  $T = 0$

These equations are quite similar to the results of the SB theory (12). In particular, the limit  $u_f \rightarrow 1$  of Eqs. (4.27) and (4.28) leads to the SB equations. Note that expectation values  $\langle n_{km}^y \rangle$  and  $\langle n_{km}^y \rangle + \langle n_{km}^x \rangle$  can be calculated similar to Eq. (4.25), see Ref. 21 for details.

#### E. Numerical solution

Note that for the analytical solution in the preceding subsection an explicit expression for the generator  $A_k^{(0)}(\epsilon; u_f)$ , was not needed. The reason was that an independent f electron energy  $u_f$  was assumed in close analogy to what is done in the well known slave boson mean field approach for the periodic Anderson model. For an improved treatment an explicit expression for  $A_k^{(0)}(\epsilon; u_f)$  should be used. Following the discussion in subsection II G we make the following ansatz for  $A_k^{(0)}(\epsilon; u_f)$

$$A_k^{(0)}(\epsilon; u_f) = \frac{\epsilon_f + D \epsilon_k + u_k - V_k}{\epsilon_f + D \epsilon_k + u_k} \quad (4.29)$$

In the limit of small  $V_k$ , we again expect an exponential decay for the hybridization  $V_k$  in this way. In Eq. (4.29),  $\epsilon_f$  denotes an energy constant to ensure a dimensionless  $A_k^{(0)}(\epsilon; u_f)$ . Note that  $A_k^{(0)}(\epsilon; u_f)$  is chosen proportional to  $V_k$  to reduce the impact of the actual value of  $V_k$  on the final results of the renormalization. Using (4.12) and (4.29) the basic renormalization equations (4.13) – (4.17) was solved numerically in Ref. 36.

FIG. 2 shows the f occupation  $n^f_i = \langle n_i^f \rangle$  as function of the bare f energy  $u_f$  at degeneracy  $u_f = 2$  for

two cases, (i) for fixed total particle occupation  $n_{\text{tot}} = n^f + n^c = 1.75$  (in red) and (ii) for fixed chemical potential (in green). Here,  $n^c = (1-N) \sum_k \langle c_k^\dagger c_k \rangle$ ;  $c_k$  is the conduction electron occupation. For the first case the result from the PRM approach shows a rather smooth decay from the integer valence region with  $n^f = 1$ , when  $\mu_f$  is located far below the Fermi level, to an empty state with no f electrons  $n^f = 0$ , when  $\mu_f$  is far above the Fermi level (black line). Note that this analytical PRM result almost completely agrees with the result from recent DMRG calculations from Ref. 37 for the same parameter values. For comparison, the figure also contains a curve obtained from the PRM approach when the chemical potential instead of  $n_{\text{tot}}$  was fixed in the calculation (red curve). Note that in this case  $n^f$  as function of  $\mu_f$  shows an abrupt change from an completely filled to an empty f state. Obviously the latter behavior can easily be understood as change of the f charge when  $\mu_f$  crosses the fixed chemical potential. In contrast, for fixed total occupation  $n_{\text{tot}}$  the Fermi level is shifted upwards, when the f level is partially depleted when  $\mu_f$  comes closer to the Fermi level. For details we refer to Ref. 36.

## V. CROSSOVER BEHAVIOR IN THE METALLIC ONE-DIMENSIONAL HOLSTEIN MODEL

In this section we discuss the one-dimensional Holstein model. As is well known, this model shows a quantum phase transition between a metallic and a charge ordered state as function of the electron-phonon coupling. In the present section we restrict ourselves to the metallic state.

Let us start with the Hamiltonian of the one-dimensional Holstein model of spinless fermions (HM) which reads,

$$H = \sum_i \left( c_i^\dagger c_i + \hbar \omega_0 \right) + \sum_{\langle ij \rangle} t_{ij} c_i^\dagger c_j + g \sum_i (b_i^\dagger + b_i) n_i \quad (5.1)$$

This model is perhaps the simplest realization of an electron-phonon (EP) system and describes the interaction between the local electron density  $n_i = c_i^\dagger c_i$  and dispersion-less phonons with frequency  $\omega_0$ . Here, the  $c_i^\dagger$  ( $b_i^\dagger$ ) denote creation operators of electrons (phonons), and the summation  $\langle ij \rangle$  runs over all pairs of neighboring lattice sites. With increasing EP coupling  $g$ , the HM undergoes the quantum phase transition from a metallic to a charge-ordered insulating state. At half-filling, the insulating state of the HM is a dimerized Peierls phase.

Because the HM is not exactly solvable, a number of different analytical and numerical methods have been applied: strong coupling expansions (38), Monte Carlo simulations (38; 39), variational (40) and renormalization group (41) approaches, exact diagonalization (ED) techniques (42), density matrix renormalization group (43; 44; 45) and dynamical mean-field theory (DMFT)

(46). However, most of these approaches are restricted in their application, and the infinite phononic Hilbert space (even for finite systems) demands the application of truncation schemes in numerical methods or involved reduction procedures.

The PRM represents an alternative analytical approach. In the following the PRM is applied to the HM where we mainly follow Refs. 32, and 33. Here we focus on the investigation of the change of physical properties by passing from the adiabatic to the anti-adiabatic limit. Furthermore, we discuss electronic and phononic quasi-particle energies as well as the impact of the system filling.

## A. Metallic solutions

For the metallic phase of the HM a very simple renormalization scheme is sufficient where only the electronic and phononic one-particle energies are renormalized.

Following Refs. 23 and 32, we make the following ansatz for the renormalized Hamiltonian

$$\begin{aligned} H &= H_0 + H_1; \\ H_0 &= \sum_k \mu_k c_k^\dagger c_k + \sum_q \omega_q b_q^\dagger b_q + E; \\ H_1 &= \frac{g}{N} \sum_{k,q} \mu_{k,q} b_q^\dagger c_{k+q}^\dagger + b_q c_{k+q}^\dagger c_k \end{aligned} \quad (5.2)$$

Here, all excitations with energies larger than a given cutoff are thought to be integrated out. Moreover, we have defined  $\mu_{k,q} = (\omega_q + \mu_k - \mu_{k+q})$ . Note that Fourier-transformed one-particle operators have been used for convenience. Next, all transitions within the energy shell between  $\mu_{k,q}$  and  $\mu_{k+q}$  will be removed by use of a unitary transformation (Eq. (2.17)),

$$H(\lambda) = e^X H e^{-X}; \quad (5.3)$$

where the following ansatz is made for the generator  $X$  of the transformation

$$X = \frac{1}{N} \sum_{k,q} A_{k,q}(\lambda) b_q^\dagger c_{k+q}^\dagger + b_q c_{k+q}^\dagger c_k \quad (5.4)$$

The part  $P(\lambda) X$  has been set equal to zero. Therefore  $A_{k,q}(\lambda)$  reads

$$A_{k,q}(\lambda) = A_{k,q}^0(\lambda) \mu_{k,q} [\omega_{k,q} - \omega_{k+q}]:$$

As before, the ansatz (5.4) is suggested by the form of the first order expression (2.20) of the generator  $X$ . Later, the coefficients  $A_{k,q}^0(\lambda)$  will be fixed in a way that  $Q(\lambda) H(\lambda) = 0$  is fulfilled, so that  $H(\lambda)$  contains no transitions larger than the new cutoff.

By evaluating (5.3), terms with four fermionic and bosonic one-particle operators and higher order terms

are generated. In order to restrict the renormalization scheme to the terms included in the ansatz (5.2), a factorization approximation has to be employed,

$$\begin{aligned} c_k^y c_k^y c_q c_q &= c_k^y c_k^y c_q c_q i + h c_k^y c_k^y c_q c_q c_q c_q \\ &= h c_k^y c_k^y i h c_q^y c_q^y c_q c_q i; \\ b_q^y b_q^y c_k^y c_k^y &= h b_q^y b_q^y c_k^y c_k^y i + h c_q^y b_q^y c_k^y c_k^y c_k^y c_k^y i \\ &= h b_q^y b_q^y i h c_k^y c_k^y c_k^y c_k^y i; \end{aligned}$$

In this way, it is possible to sum up the series expansion from transformation (5.3).

The parameters  $A_{k;q}^0(\epsilon; \epsilon)$  as well as the renormalization equations for  $\mu_k, \mu_q, g_{k;q},$  and  $E$  can be found by comparing the final result obtained from the explicit evaluation of the unitary transformation (5.3) with the renormalization ansatz (5.2), where  $\epsilon$  is replaced by  $\epsilon$ . The result is given in Ref. 23. It can be further simplified in the thermodynamic limit  $N \rightarrow \infty$ . By expanding the renormalization equations from Ref. 23 in powers of  $g$ , one finds that only terms of quadratic or linear order in  $g$  survive. The final equations read

$$\begin{aligned} \mu_k(\epsilon) - \mu_k &= \\ &= \frac{1}{N} \sum_q n_q^b + n_{k+q}^c \frac{g^2 \epsilon_{k;q}(\epsilon; \epsilon)}{\epsilon_q + \mu_k - \mu_{k+q}} \\ &\quad - \frac{1}{N} \sum_q n_q^b - n_{k-q}^c + 1 \frac{g^2 \epsilon_{k;q}(\epsilon; \epsilon)}{\epsilon_q + \mu_k - \mu_{k-q}}; \end{aligned} \quad (5.5)$$

$$\begin{aligned} \epsilon_q(\epsilon) - \epsilon_q &= \\ &= \frac{1}{N} \sum_k n_k^c - n_{k+q}^c \frac{g^2 \epsilon_{k;q}(\epsilon; \epsilon)}{\epsilon_q + \mu_k - \mu_{k+q}} \end{aligned} \quad (5.6)$$

where  $n_k^c = h c_k^y c_k^y i$ ,  $n_q^b = h b_q^y b_q^y i$ , and  $\epsilon_{k;q}(\epsilon; \epsilon) = \epsilon_{k;q}[\epsilon_{k;q}, \epsilon_{k;q}]$ .

Note that the renormalization equations still depend on unknown expectation values  $h c_k^y c_k^y i$  and  $h b_q^y b_q^y i$  which follow from the factorization approximation. Following Ref. 32, they are best evaluated with respect to the full Hamiltonian  $H$ .

Exploiting  $h A_i i = \lim_{\epsilon \rightarrow 0} h A_i i_\epsilon$ , we derive additional renormalization equations for the fermionic and bosonic one-particle operators,  $c_k^y$  and  $b_q^y$ . They have the following form according to Refs. 23 and 33,

$$c_k^y = c_k^y + \sum_q \epsilon_{k;q} c_{k+q}^y b_q^y + \epsilon_{k;q} c_k^y b_q^y; \quad (5.7)$$

$$b_q^y = b_q^y + \sum_k \epsilon_{k;q} c_{k+q}^y c_k^y; \quad (5.8)$$

The set of renormalization equations has to be solved self-consistently: One chooses some values for the expectation values. With these values, the numerical evaluation starts from the cutoff of the original model  $H$  and

proceeds step by step to  $\epsilon = 0$ . For  $\epsilon = 0$ , the Hamiltonian and the one-particle operators are fully renormalized. The case  $\epsilon = 0$  allows the re-calculation of all expectation values, and the renormalization procedure starts again with the improved expectation values by reducing again the cutoff from  $\epsilon$  to  $\epsilon = 0$ . After a sufficient number of such cycles, the expectation values are converged and the renormalization equations are solved self-consistently. Thus, we finally obtain an effectively free model,

$$H = \sum_k \mu_k c_k^y c_k^y + \sum_q \epsilon_q b_q^y b_q^y + E; \quad (5.9)$$

where we have introduced the renormalized dispersion relations  $\mu_k = \lim_{\epsilon \rightarrow 0} \mu_k$  and  $\epsilon_q = \lim_{\epsilon \rightarrow 0} \epsilon_q$ , and the energy shift  $E = \lim_{\epsilon \rightarrow 0} E$ .

For the numerical evaluation of the renormalization equations we choose a lattice size of  $N = 1000$  sites. The temperature is fixed to  $T = 0$ .

#### B. Adiabatic case

At first, let us discuss our results for the so-called adiabatic case  $\epsilon_0 \rightarrow 0$ . They are shown in panel (a) of Figs. 3, 4, 5, and in panels (a) and (b) of Fig. 6. First, according to Fig. 3a the phononic quasi-particle energies  $\epsilon_q$  (half-lling) are found to gain dispersion due to the coupling between electronic and phononic degrees of freedom in particular around  $q = \pi$ . Furthermore, if the coupling exceeds a critical value  $g_c$  non-physical negative energies at  $q = \pi$  occur. This feature signals the break-down of the present description for the metallic phase at the quantum phase transition to the insulating Peierls state.

Whereas at half-lling the phonon softening occurs at the Brillouin-zone boundary, soft phonon modes are found at  $2k_F = 2\pi/3$  and at  $2k_F = \pi/2$  for lling  $1/3$  and  $1/4$ , respectively. This can be seen in Fig. 6. Since the phonon softening can be considered as a precursor effect of the metal-insulator transition, the type of the broken symmetry in the insulating phase strongly depends on the lling of the electronic band. Note that the critical EP coupling  $g_c$  of the phase transition may be determined from the vanishing of the phonon mode (see Ref. 23).

At half-lling and for  $\epsilon_0 = 0.1t$ , a value of  $g_c = 0.31t$  is found, which is somewhat larger than the DMRG result of  $g_c = 0.28t$  of Refs. 43 and 45. In subsection VIA the determination of the critical coupling  $g_c$  within our PRM approach will be discussed in more detail.

Fig. 4a shows the phonon distribution  $n_q^b = h b_q^y b_q^y i$  for the same parameter values as in Fig. 3a. There are two pronounced maxima found at wave numbers  $q = \pi$  and  $q = 0$ . The peak at  $q = \pi$  is directly connected to the softening of  $\epsilon_q$  at the zone boundary and can therefore be considered as a precursor of the transition to a dimerized state. For the critical EP coupling  $g = g_c$  a divergency of  $n_q^b$  should appear at  $q = \pi$ . The second peak around  $q = 0$  follows from renormalization contributions which

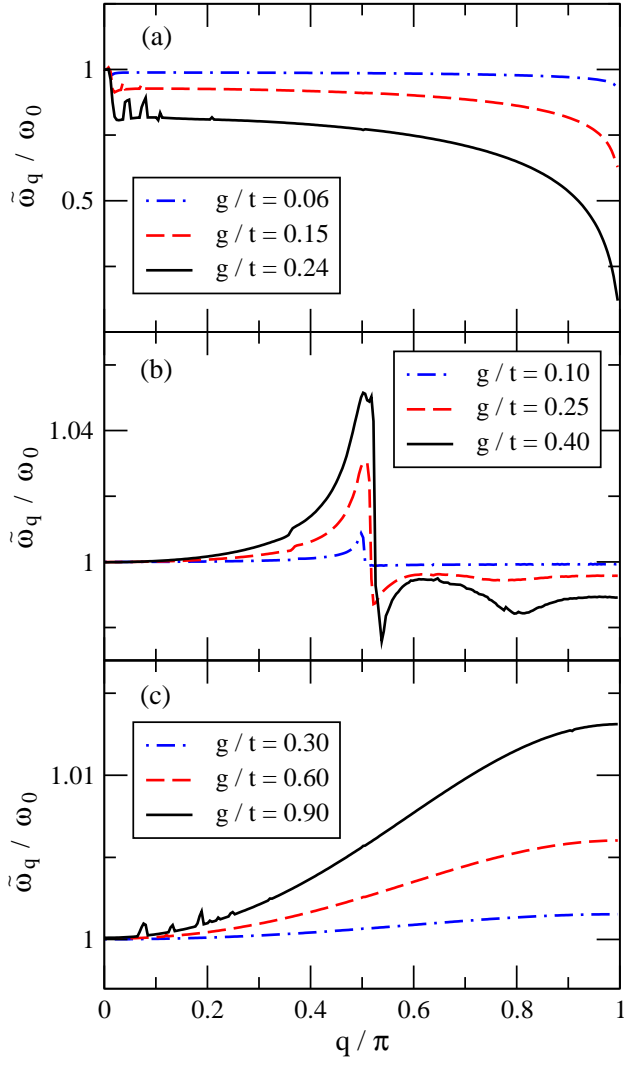


FIG. 3 (Color online) Bosonic quasiparticle energies  $\tilde{\omega}_q = \omega_0$  at half-filling as function of  $q$  for different values of the EP coupling  $g$  in the adiabatic case  $\omega_0/t = 0.05$  (panel (a)), the intermediate case  $\omega_0/t = 2.8$  (panel (b)), and the anti-adiabatic case  $\omega_0/t = 6.0$  (panel (c)).

become strong for small  $q$  for the adiabatic case  $\omega_0/t \rightarrow 0$ . This will be explained in more detail in the discussion part below.

Finally, in Fig. 5a the renormalized fermionic one-particle energy  $\tilde{\epsilon}_k$  is shown in relation to the original dispersion  $\epsilon_k = -2t \cos ka$  for the same parameter values as in Fig. 3a. Though the absolute changes are quite small, the difference between  $\tilde{\epsilon}_k$  and  $\epsilon_k$  is strongest in the vicinity of  $k = 0$  and  $k = \pi$ . In particular, we find  $\tilde{\epsilon}_k < \epsilon_k$  for  $k = 0$  and  $\tilde{\epsilon}_k > \epsilon_k$  for  $k = \pi$ , so that the renormalized bandwidth becomes larger than  $4t$ , i.e. larger than the original bandwidth.

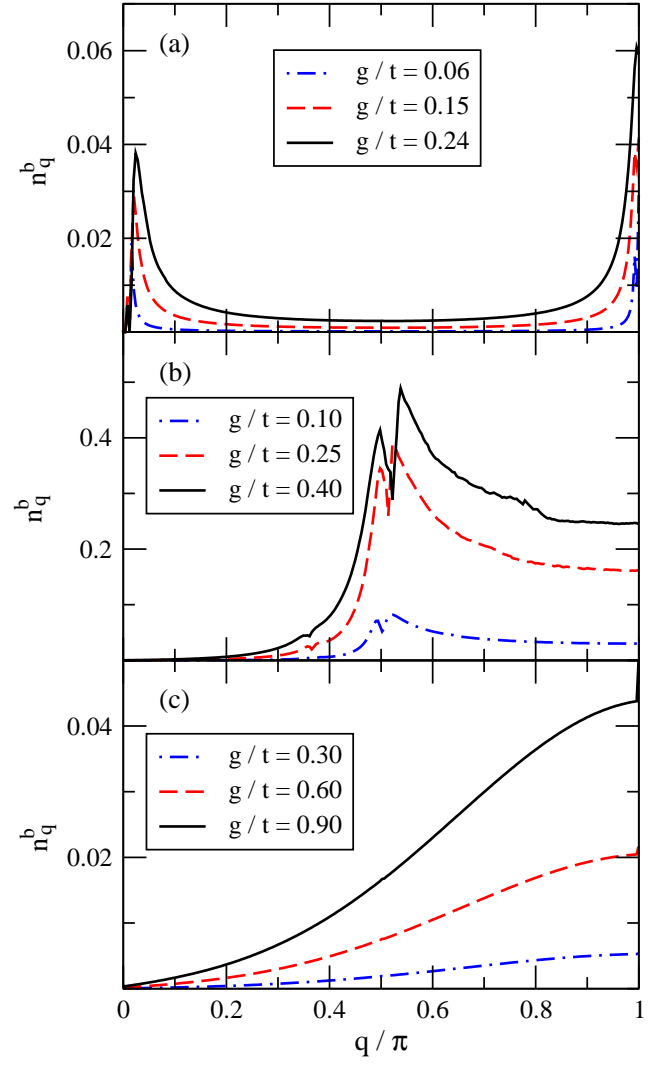


FIG. 4 (Color online) Phonon distribution  $n_q^b = \langle b_q^\dagger b_q \rangle$  as function of  $q$  for the same parameters as in Fig. 3.

### C. Intermediate case

Next, let us discuss the results for phonon frequencies  $\omega_0$  of the order of the hopping matrix element  $t$  (intermediate case). The results are found in the panels (b) of Figs. 3, 4, 5. In contrast to the adiabatic case, the renormalized phonon energy  $\tilde{\omega}_q$  (Fig. 3b) now shows a noticeable 'kink' at an intermediate wave vector (for  $\omega_0/t = 2.8$ ). This particular  $q$  value, which will be called  $q_k$  in the following strongly depends on the initial phonon energy  $\omega_0$ . The appearance of such a 'kink' at  $q_k < \pi$  is a specific feature of the intermediate case. The wave number  $q_k$  is characterized by a strong renormalization of the phonon energy in a small  $q$ -range around  $q_k$ , where  $\tilde{\omega}_q = \omega_0 > 1$  for  $q < q_k$  and  $\tilde{\omega}_q = \omega_0 < 1$  for  $q > q_k$  holds. The origin of these features will be discussed in more detail below.

Similar to  $\tilde{\omega}_q$ , also the phonon distribution  $n_q^b$  in

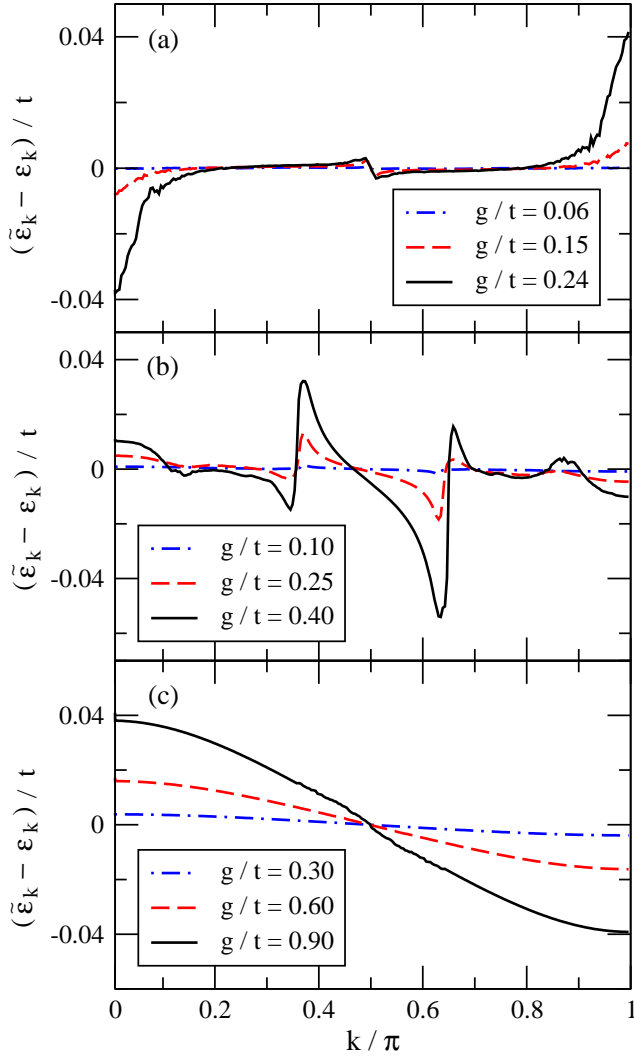


FIG. 5 (Color online) Fermionic quasi-particle energies  $(\tilde{\epsilon}_k - \epsilon_k)/t$  as function of  $k$  for the same parameters as in Fig. 3. Here  $\epsilon_k$  is the original electronic dispersion.

Fig. 4b shows a pronounced structure of considerable weight around  $q_k$ . Finally, in Fig. 5b the difference of the fermionic one-particle energies  $(\tilde{\epsilon}_k - \epsilon_k)$  is shown. Again a remarkable structure is found, though the absolute changes are small for the present  $g$ -values.

#### D. Anti-adiabatic case

Finally, let us discuss the results for the anti-adiabatic case  $\epsilon_0 = t$ . In panels (c) of Figs. 3, 4, 5 a value of  $\epsilon_0 = t = 6.0$  was used. A most important feature a stiffening of the renormalized phonon frequency  $\omega_q$  (Fig. 3c) is found instead of a softening as in the adiabatic case. In particular, for large values of the EP coupling no softening of the phonon modes is found at  $q = \pi$ . Moreover, no large renormalization contributions occur in any limited

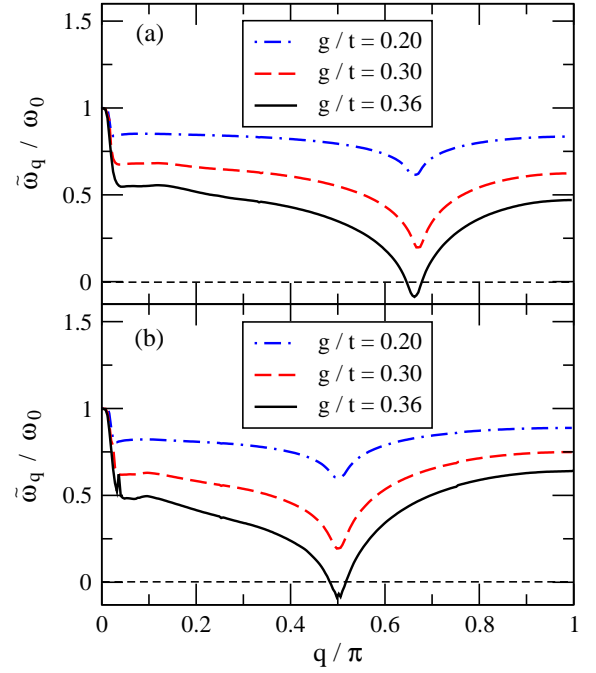


FIG. 6 (Color online) (a) Phononic quasi-particle energy  $\omega_q$  in unit of  $\omega_0$  of the one-dimensional HM with 500 lattice sites for filling 1/3 and different values of the EP coupling  $g$ .  $\epsilon_0 = t = 0.05$ . (b) Same quantity  $\omega_q = \omega_0$  for filling 1/4.

$q$ -space regime which would lead to peak-like structures. Instead an overall smooth behavior is found in the entire Brillouin zone.

Also the phonon distribution  $n_q^b$  (Fig. 4c) shows a smooth behavior with a maximum at  $q = \pi$ . The lack of strong peak-like structures in  $q$  space indicates that there is no phonon mode that gives a dominant contribution to the renormalization processes.

If one compares the renormalized electronic bandwidth for the anti-adiabatic case (Fig. 5c) with that of the adiabatic case (Fig. 5a), one observes a relatively strong reduction of the bandwidth. This indicates the tendency to localization in the anti-adiabatic case. It also indicates that the metal-insulator transition in the anti-adiabatic limit can be understood as the formation of small immobile polarons with electrons surrounded by clouds of phonon excitations. In the present PRM approach, a renormalized one-particle excitation like  $\tilde{\epsilon}_k$  corresponds to a quasiparticle of the coupled many-particle system. Therefore, a completely flat  $k$  dependence of  $\tilde{\epsilon}_k$  would be expected to be found in the insulating regime.

#### E. Discussion

It may be worthwhile to demonstrate that the PRM approach has the advantage that all features of the results for  $\omega_q$  and  $n_q^b$  or  $\tilde{\epsilon}_k$  can easily be understood on the basis of the former renormalization equations. For simplicity,

we shall restrict ourselves to the case of half-filling and to the renormalization of the phonon energies  $\epsilon_q$ .

The basic equation is the renormalization equation (5.6). Due to the  $\delta$ -functions  $\delta(k, q; \pm)$  in all equations a renormalization approximately occurs when the energy difference  $|\epsilon_q + \epsilon_k; \epsilon_{k+q}|$  lies within a small energy shell between  $\epsilon_k$  and  $\epsilon_{k+q}$ . As one can see from (5.6) the most dominant renormalization processes take place for small values of the cutoff  $\epsilon_c$ . Therefore, the largest renormalization contributions come from  $k$  and  $q$  values that fulfill the condition

$$|\epsilon_{k+q} - \epsilon_k - \epsilon_q| < \epsilon_c \quad (5.10)$$

From (5.6) directly follows a second condition for the renormalization contributions to  $\epsilon_q$ . Due to the expectation values  $(n_k^c - n_{k+q}^c)$  in (5.6) the renormalization of  $\epsilon_q$  is caused from the coupling to particle-hole excitations. Therefore, the energies  $\epsilon_k$  and  $\epsilon_{k+q}$  have to be either below or above the Fermi level, i.e.  $|k| < k_F$  and  $|k+q| > k_F$  or  $|k| > k_F$  and  $|k+q| < k_F$ .

Let us first discuss the adiabatic case  $\epsilon_0 \rightarrow 0$ . The most dominant contributions to the renormalization are expected when both conditions are simultaneously fulfilled. This is the case for  $q = 0$  or partially also for  $q \neq 0$ . Note that for  $q = 0$  practically all  $k$ -values can contribute to the renormalization of (5.6), which is not the case for  $q$ -values different from 0. For instance, for  $q \neq 0$  only few  $k$  points from the sum in (5.6) can contribute which are located in a small region around the Fermi momentum  $k_F$ . On the other hand, for  $q = 0$ , the energy denominator is almost zero so that still some noticeable renormalization structures are found in Fig. 3a. Moreover, for the adiabatic case, where  $\epsilon_q$  is small, the energy denominator of (5.6) can be replaced by  $(\epsilon_k - \epsilon_{k+q})$ . Therefore, almost all particle-hole contributions to  $\epsilon_q$  are negative because  $(n_k^c - n_{k+q}^c)$  and  $(\epsilon_k - \epsilon_{k+q})$  have always different signs. One concludes that in the adiabatic case  $\epsilon_q$  will be renormalized to smaller values where the renormalization at  $q = 0$  should be dominant.

The behavior of  $\epsilon_q$  for the case of intermediate phonon frequencies ( $\epsilon_0 \rightarrow 2.8$  in Fig. 3b and Fig. 4b) can again be understood on the basis of the renormalization equations (5.6) and condition (5.10). As was already discussed, particle-hole excitations lead to the renormalization of  $\epsilon_q$ . Therefore, from the sum over  $k$  in Eq. (5.6) only  $k$  terms contribute where either  $|k| < k_F$  and  $|k+q| > k_F$  or  $|k| > k_F$  and  $|k+q| < k_F$ . For the latter case always  $(\epsilon_k - \epsilon_{k+q}) > 0$  is valid so that (5.10) can not be fulfilled. Therefore, we can restrict ourselves to contributions  $|k| < k_F$  und  $|k+q| > k_F$ , for which always  $(\epsilon_k - \epsilon_{k+q}) < 0$  and  $(n_k^c - n_{k+q}^c) > 0$  holds. The largest renormalization should result from a small  $q$  region around some  $q$ -vector  $q_k$  for which  $\epsilon_{k+q_k} - \epsilon_k = \epsilon_0$  is approximately fulfilled. Since  $\epsilon_0$  is of the order of  $t$ ,  $q_k$  is located somewhere in the middle of the Brillouin zone and depends strongly on  $\epsilon_0$ . From Eq. (5.6) also follows that renormalization contributions to  $\epsilon_q$  change

their sign at  $q_k$  due to the sign change in the energy denominator.

Finally, from equation (5.6) one may point out also the stiffening of the phonon modes in the anti-adiabatic case  $\epsilon_0 \rightarrow 6.0$ . In this case the phonon energy  $\epsilon_0$  is much larger than the electronic bandwidth. Therefore, for all a positive energy denominator  $(\epsilon_q + \epsilon_k - \epsilon_{k+q})$  is obtained. Nevertheless, for half-filling in the  $k$  sum on the right hand side of (5.6) there are as many negative as positive terms due to the factor  $(n_k^c - n_{k+q}^c)$ . Since from  $(n_k^c - n_{k+q}^c) < 0$  always follows  $(\epsilon_k - \epsilon_{k+q}) > 0$ , the negative terms have larger energy denominators and are always smaller than the positive terms. The resulting renormalization of  $\epsilon_q$  is therefore positive for all  $q$  values and largest for  $q = 0$  due to the smallest energy denominator.

## VI. QUANTUM PHASE TRANSITION IN THE ONE-DIMENSIONAL HOLSTEIN MODEL

In this section we want to demonstrate the ability of the PRM approach to describe also quantum phase transitions. In particular, we shall investigate the transition from the metallic to the insulating charge ordered phase when the electron-phonon coupling  $g$  exceeds a critical value.

### A. Uniform description of metallic and insulating phases at half-filling

In the following we present a uniform description that covers the metallic as well as the insulating phase of the HM in the adiabatic case. We mainly follow the approach of Ref. 32 where we have discussed methodological aspects in more detail. As already mentioned above, the simple approach of subsection V A breaks down for EP couplings  $g$  larger than some critical value  $g_c$  where a long-range charge density wave occurs and the ions are shifted away from their symmetric positions. An adequate theoretical description needs to take into account a broken symmetry field. For this purpose, the underlying idea of subsection III C to take such a term into account in the renormalization ansatz will be transferred to the present case. As one can see from Fig. 6, the order parameter of the insulating phase strongly depends on the filling of the electronic band. Therefore, in the following we restrict ourselves to the case of half-filling. Here, the unit cell is doubled and a dimerization occurs in the insulating phase.

Following Ref. 32, the Hamiltonian in the reduced Brillouin

Brillouin zone including symmetry breaking fields reads

$$\begin{aligned}
 H &= H_0 + H_1; \\
 H_0 &= \sum_{k>0} \sum_{q>0} \left( \sum_{\mathbf{k}} c_{\mathbf{k}}^y c_{\mathbf{k}} + \sum_{\mathbf{q}} b_{\mathbf{q}}^y b_{\mathbf{q}} \right) \\
 &+ E + \sum_{\mathbf{k}} \left( c_{\mathbf{k}}^y c_{\mathbf{k}} + h c_{\mathbf{k}} \right) \\
 &+ \frac{P}{N} \sum_{\mathbf{k}} b_{\mathbf{k}}^y b_{\mathbf{k}} + h c_{\mathbf{k}}; \\
 H_1 &= \frac{1}{N} \sum_{\mathbf{k}, \mathbf{q}} \sum_{\mathbf{i}, \mathbf{j}} g_{\mathbf{k}, \mathbf{q}}^{i, j} (b_{\mathbf{q}}^y) (c_{\mathbf{k}}^y c_{\mathbf{k}+\mathbf{q}}) + h c_{\mathbf{k}};
 \end{aligned} \quad (6.1)$$

where  $c_{\mathbf{k}}^y$  and  $b_{\mathbf{k}}^y$  are the appropriate order parameters for the electronic and the phononic symmetry breaking fields. Note that the reduced Brillouin zone leads to additional band indices  $i, j = 0, 1$  of both electronic and phononic one-particle operators. Furthermore, we defined  $A = A_{\mathbf{k}}^i$  and  $Q = Q_{\mathbf{k}}^i$ . The ansatz (6.1) is restricted to the one-dimensional case at half-filling. To extend the approach to higher dimensions one would need to take into account all  $Q$  wave vectors of the Brillouin zone boundary.

Before we can proceed we need to diagonalize  $H_0$ . For this purpose a rotation in the fermionic subspace and a translation to new ionic equilibrium positions are performed in order to diagonalize  $H_0$ ;

$$\begin{aligned}
 H_0 &= \sum_{\mathbf{k}} \sum_{\mathbf{q}} \left( c_{\mathbf{k}}^y c_{\mathbf{k}} + c_{\mathbf{q}}^y c_{\mathbf{q}} + b_{\mathbf{q}}^y b_{\mathbf{q}} \right) \\
 &+ \sum_{\mathbf{k}} \sum_{\mathbf{q}} \left( c_{\mathbf{k}}^y c_{\mathbf{k}+\mathbf{q}} + b_{\mathbf{q}}^y b_{\mathbf{q}} \right) + E
 \end{aligned} \quad (6.2)$$

with new fermionic and bosonic creation and annihilation operators,  $c_{\mathbf{k}}^{(y)}$  and  $b_{\mathbf{q}}^{(y)}$ , and we rewrite  $H_1$  in terms of the new operators,  $c_{\mathbf{k}}^{(y)}$  and  $b_{\mathbf{q}}^{(y)}$ .

Finally, we have to transform  $H$  to  $H'$  according to (2.17) to derive the renormalization equations for the parameters of  $H'$ . Here the ansatz

$$\begin{aligned}
 c_{\mathbf{k}}^{(y)} &= \frac{1}{N} \sum_{\mathbf{k}, \mathbf{q}} \sum_{\mathbf{i}, \mathbf{j}} A_{\mathbf{k}, \mathbf{q}}^{i, j} c_{\mathbf{k}}^y \\
 b_{\mathbf{q}}^{(y)} &= \sum_{\mathbf{k}} \left( c_{\mathbf{k}}^y c_{\mathbf{k}+\mathbf{q}} \right) + h c_{\mathbf{k}}
 \end{aligned}$$

is used. The coefficients  $A_{\mathbf{k}, \mathbf{q}}^{i, j}$  have to be fixed in such a way so that only excitations with energies smaller than  $(\epsilon_{\mathbf{k}})$  contribute to  $H_1$ . The renormalization equations for the parameters  $\sum_{\mathbf{k}} c_{\mathbf{k}}^y c_{\mathbf{k}}; \sum_{\mathbf{q}} b_{\mathbf{q}}^y b_{\mathbf{q}}; \sum_{\mathbf{k}} c_{\mathbf{k}}^y c_{\mathbf{k}+\mathbf{q}}; \sum_{\mathbf{k}} b_{\mathbf{k}}^y b_{\mathbf{k}}$  and  $g_{\mathbf{k}, \mathbf{q}}^{i, j}$  are finally obtained by comparison with (6.1) after the creation and annihilation operators  $c_{\mathbf{k}}^{(y)}; b_{\mathbf{q}}^{(y)}$  have been transformed back to the original operators  $c_{\mathbf{k}}^y; b_{\mathbf{q}}^y$ . The actual calculations are done in close analogy to subsection V A. Note that again a factorization approximation was used and only operators of the same

structure as in (6.1) are kept. Therefore, the renormalization equations still depend on unknown expectation values, which are evaluated with the full Hamiltonian  $H$ . Note that in order to evaluate the expectation values  $\langle H \rangle = \langle H_{\text{eff}} \rangle$  additional renormalization equations have also to be found for the fermionic and bosonic one-particle operators,  $c_{\mathbf{k}}^y$  and  $b_{\mathbf{q}}^y$ . By using the same approximations as for the Hamiltonian a resulting set of renormalization equations is derived. It is solved numerically where the equations for the expectation values are taken into account in a self-consistency loop.

By eliminating all excitations in steps we finally arrive at  $\epsilon_{\mathbf{k}} = 0$  which again provides an effectively free model  $H' = \lim_{\epsilon_{\mathbf{k}} \rightarrow 0} H = \lim_{\epsilon_{\mathbf{k}} \rightarrow 0} H_0$ . It reads

$$\begin{aligned}
 H' &= \sum_{\mathbf{k}} \sum_{\mathbf{q}} \left( c_{\mathbf{k}}^y c_{\mathbf{k}} + c_{\mathbf{q}}^y c_{\mathbf{q}} + b_{\mathbf{q}}^y b_{\mathbf{q}} \right) \\
 &+ \sum_{\mathbf{k}} \sum_{\mathbf{q}} \left( c_{\mathbf{k}}^y c_{\mathbf{k}+\mathbf{q}} + b_{\mathbf{q}}^y b_{\mathbf{q}} \right) + E
 \end{aligned} \quad (6.3)$$

where it was defined  $\sum_{\mathbf{k}} c_{\mathbf{k}}^y c_{\mathbf{k}} = \lim_{\epsilon_{\mathbf{k}} \rightarrow 0} \sum_{\mathbf{k}} c_{\mathbf{k}}^y c_{\mathbf{k}}$ ,  $\sum_{\mathbf{q}} b_{\mathbf{q}}^y b_{\mathbf{q}} = \lim_{\epsilon_{\mathbf{q}} \rightarrow 0} \sum_{\mathbf{q}} b_{\mathbf{q}}^y b_{\mathbf{q}}$ , and  $\sum_{\mathbf{k}} c_{\mathbf{k}}^y c_{\mathbf{k}+\mathbf{q}} = \lim_{\epsilon_{\mathbf{k}} \rightarrow 0} \sum_{\mathbf{k}} c_{\mathbf{k}}^y c_{\mathbf{k}+\mathbf{q}}$ . Note that all excitations from  $H_1$  were used up to renormalize the parameters of  $H_0$ . The expectation values are also calculated in the limit  $\epsilon_{\mathbf{k}} \rightarrow 0$ . Because  $H'$  is a free model they can easily be determined from  $\langle H \rangle = \langle H_{\text{eff}} \rangle = h(\lim_{\epsilon_{\mathbf{k}} \rightarrow 0} A)_{\text{eff}}$ :

## B. Results

In the following, we first demonstrate that the PRM can be used to investigate the Peierls transition of the one-dimensional spinless Holstein model (5.1) at half-filling. The phonon energy is fixed to  $\epsilon_0 = 0.1t$ . In particular, our analytical approach provides a simultaneous theoretical description for both the metallic and the insulating phase. Finally, we compare our results with recent DMRG calculations 43; 45.

First, let us consider the critical electron-phonon coupling  $g_c$ . For that purpose, in Fig. 7 a characteristic electronic excitation gap  $\tilde{\epsilon}$  for finite system size is plotted as function of the EP coupling  $g$ , where  $\tilde{\epsilon}$  was determined from the opening of a gap in the quasi-particle energy  $\epsilon_{\mathbf{k}}$  (see text below). A closer inspection of the data shows that an insulating phase with a finite excitation gap is obtained for  $g$  values larger than the critical EP coupling  $g_c = 0.24t$ . A comparison with the critical value  $g_c = 0.28t$  obtained from DMRG calculations 43; 45 shows that the critical values from the PRM approach might be somewhat too small. However, this difference can be attributed to the exploited factorization approximation in the PRM which suppresses fluctuations so that the ordered insulating phase is stabilized. Note that in order to determine  $g_c$  a careful finite-size scaling was performed as shown for some  $g$  values in the inset of Fig. 7. A linear regression was applied to extrapolate our results to infinite system size. Note that the finite

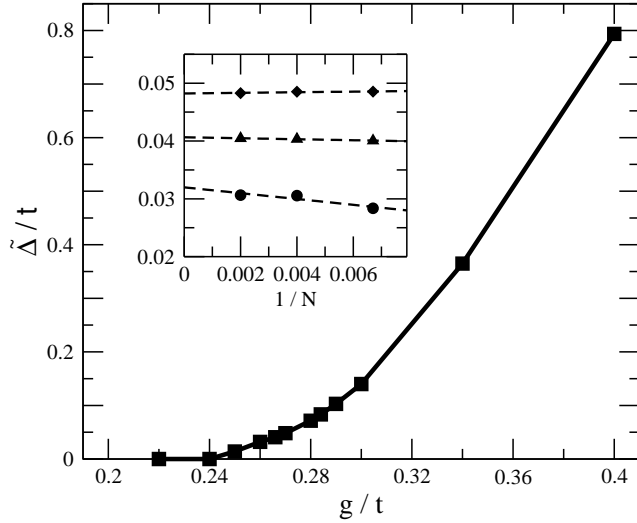


FIG. 7 Electronic excitation gap of the one-dimensional HM at half-filling where the data are extrapolated to an infinite chain. The inset shows the finite-size scaling for  $g$  values of the EP coupling of 0.26t (circles), 0.266t (triangles), and 0.27t (diamonds).

size scaling may be affected by two different effects: Suppression of long-range fluctuations by the finite cluster size and by the used factorization approximation so that a rather unusual dependence on the system size is found.

In contrast to other methods, the PRM directly provides the quasi-particle energies: After the renormalization equations were solved self-consistently the electronic and phononic quasi-particle energies of the system,  $\epsilon_k$  and  $\omega_q$ , respectively, are given by the limit  $\beta \rightarrow 0$  of the parameters  $\epsilon_{jk}^C$  and  $\omega_{qj}^B$  of the diagonal Hamiltonian  $H_{0j}(\beta \rightarrow 0)$  of (6.2). In Fig. 8 the renormalized one-particle energies  $\epsilon_k = \epsilon_{jk}^C = 0$  and  $\omega_q = \omega_{qj}^B = 0$  as quasi-particle of the full system are shown for different values of the EP coupling  $g$ . The upper panel shows that the electronic one-particle energies depend only slightly on  $g$  as long as  $g$  is smaller than the critical value  $g_c \approx 0.24t$ . If the EP coupling  $g$  is further increased a gap  $\sim$  opens at the Fermi energy so that the system becomes an insulator. Remember that the gap  $\sim$  has been used as order parameter to determine the critical EP coupling  $g_c$  of the metal-insulator transition (see Fig. 7). The lower panel of Fig. 8 shows the results for the phononic one-particle energy  $\omega_q$ . One can see that  $\omega_q$  gains dispersion due to the coupling  $g$  between the electronic and phononic degrees of freedom. In particular, the phonon mode at momentum  $2k_F$ , i.e. at the Brillouin-zone boundary becomes soft if the EP coupling is increased up to  $g_c \approx 0.24t$ . However, in contrast to the metallic solution of subsection V A  $\omega_q$  at  $2k_F$  always remains positive though it is very small. Note that for  $g$  values larger than  $g_c$  the energy  $\omega_q$  increases again. This phonon softening at the phase transition has to be interpreted as a lattice instability which leads to the formation of the insulating Peierls state for

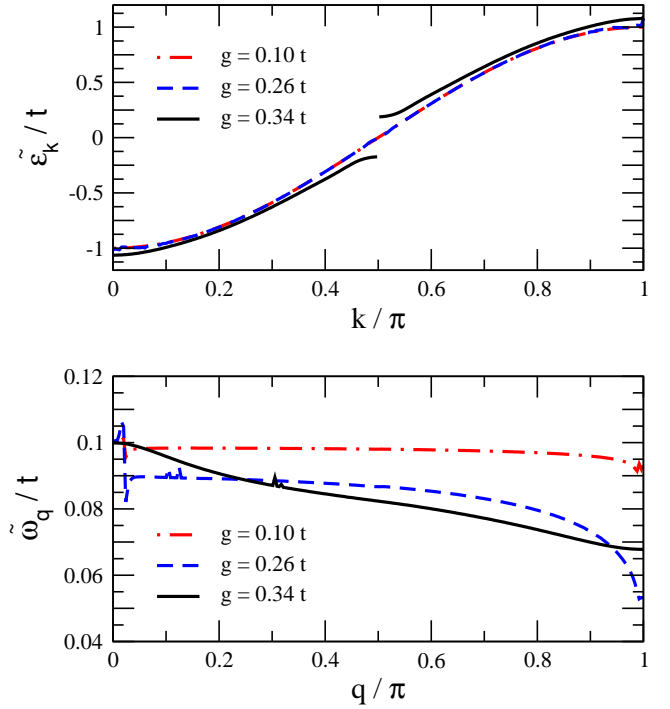


FIG. 8 (Color online) Fermionic quasi-particle energy  $\epsilon_k = \epsilon_{jk}^C = 0$  (upper panel) and bosonic quasi-particle energy  $\omega_q = \omega_{qj}^B = 0$  (lower panel) of a chain with 500 lattice sites for different EP couplings  $g$ .

$g > g_c$ . The phase transition is associated with a shift of the ionic equilibrium positions. A lattice stiffening occurs if  $g$  is further increased to values much larger than the critical value  $g_c \approx 0.24t$ .

Note also that the critical coupling  $g_c \approx 0.24t$  obtained from the opening of the gap in  $\epsilon_k$  is significantly smaller than the  $g_c$  value of  $\approx 0.31t$  which was found from the vanishing of the phonon mode at the Brillouin zone boundary in the metallic solution of subsection V A. Instead, one would expect that both the gap in  $\epsilon_k$  and the vanishing of  $\omega_q$  should occur at the same  $g_c$  value. This inconsistency can again be understood from the factorization approximation in the PRM: As discussed above, the inclusion of additional fluctuations leads to a less stable insulating phase so that a  $g_c$  value larger than  $0.24t$  would follow. On the other hand, the dispersion of  $\omega_q$  due to renormalization processes would be enhanced by taking additional fluctuations into account. Thus, a  $g_c$  value smaller than  $\approx 0.31t$  would follow. In this way, both ways to determine  $g_c$  would be consistent with each other and could lead to a common result for  $g_c$  in between  $0.24t$  and  $0.31t$ . This would be in agreement with the DMRG value of  $g_c \approx 0.28t$  (43; 45).



## VII. CHARGE ORDERING AND SUPERCONDUCTIVITY IN THE TWO-DIMENSIONAL HOLSTEIN MODEL

As a second example for a quantum phase transition, we now study the competition of charge-density waves (CDW) and superconductivity (SC) for the two-dimensional half-filled Holstein model by use of the projector-based renormalization method. In one dimension the coupling of electrons to phonons gives rise to a metal-insulator transition. In two dimensions the electron-phonon interaction may also be responsible for the formation of Cooper pairs. In the following, the competing influence of superconductivity and charge order will be discussed for two dimensions. The PRM not only allows to study SC and CDW correlation functions but gives direct access to the order parameters. The discussion closely follows the approach of Ref. 52

The relationship between a possible superconducting and an insulating Peierls-CDW phase in the 2d-Holstein model has been subject to a number of studies in the literature (for details we refer to Ref. 52). In general, it is believed that the onset of strong SC correlations suppresses the development of CDW correlations and vice versa. Thus close to the phase transition, both types of correlations must be taken into account.

### A. Unified description of SC and CDW phases at half-filling

To find a uniform description of both the superconducting (SC) and the insulating CDW phase, two fields, which break the translation and the gauge symmetry should be added to the Hamiltonian. Thus, the model on a square Lattice is given by

$$H = H_0 + H_1 \quad (7.1)$$

$$H_0 = \sum_{\mathbf{k};} \left( \epsilon_{\mathbf{k}} c_{\mathbf{k}}^\dagger c_{\mathbf{k}} + \epsilon_0 \sum_{\mathbf{q}} b_{\mathbf{q}}^\dagger b_{\mathbf{q}} \right) + \sum_{\mathbf{k}} \left( s_{\mathbf{k}} c_{\mathbf{k}}^\dagger c_{\mathbf{k}+\mathbf{Q}}^\dagger + s_{\mathbf{k}} c_{\mathbf{k}+\mathbf{Q}} c_{\mathbf{k}} \right) + \frac{1}{2} \sum_{\mathbf{k};} \left( p_{\mathbf{k}} c_{\mathbf{k}}^\dagger c_{\mathbf{k}+\mathbf{Q}} + \text{h.c.} + \frac{p_{-\mathbf{k}}}{N} (b_{\mathbf{Q}}^\dagger + b_{\mathbf{Q}}) \right) \quad (7.2)$$

$$H_1 = \frac{1}{N} g \sum_{\mathbf{k}, \mathbf{q};} \left( b_{\mathbf{q}}^\dagger c_{\mathbf{k}}^\dagger c_{\mathbf{k}+\mathbf{q}} + b_{\mathbf{q}} c_{\mathbf{k}+\mathbf{q}} c_{\mathbf{k}} \right) \quad (7.3)$$

where  $\mathbf{k}$  is the wave vector on the reciprocal lattice and  $\mathbf{Q}$  is the characteristic wave vector of the CDW phase  $\mathbf{Q} = (\pi/a, \pi/a)$ . Assuming an electron hopping between nearest-neighbor sites, the electronic dispersion is given by  $\epsilon_{\mathbf{k}} = 2t(\cos k_x a + \cos k_y a)$ , where  $t$  is the chemical potential. Moreover,  $\epsilon_0$  is the dispersionless phonon energy, and  $g$  denotes the coupling strength between the electrons and phonons. At the beginning of the renormalization the two symmetry breaking fields  $s_{\mathbf{k}}$  and  $p_{\mathbf{k}}$ ,

as well as  $b$ , are assumed to be infinitesimally small ( $s_{\mathbf{k}} \rightarrow 0$ ,  $p_{\mathbf{k}} \rightarrow 0$ ;  $b \rightarrow 0$ ).

The unperturbed Hamiltonian  $H_0$  can be diagonalized, since its electronic part is quadratic in the fermionic operators. Note that due to the doubling of the unit cell in the insulating phase, in  $H_0$  the creation operator  $c_{\mathbf{k}}^\dagger$  is coupled to  $c_{\mathbf{k}+\mathbf{Q}}$ . In addition the coupling of  $c_{\mathbf{k}}^\dagger$  to  $c_{\mathbf{k}+\mathbf{Q}}^\dagger$  is caused by superconductivity. Therefore, the eigenmodes of  $H_0$  can be represented as a linear combination of the following four operators

$$c_{\mathbf{k}+\mathbf{Q}}^\dagger, c_{\mathbf{k}}^\dagger, c_{\mathbf{k}+\mathbf{Q}}, c_{\mathbf{k}} \quad (7.4)$$

In the renormalization procedure, all transitions with energies larger than  $\omega$  will be integrated out. As can be seen, the renormalized Hamiltonian can again be divided into  $H = H_0 + H_1$ . If one denotes by  $a_{\mathbf{k};}^\dagger$  ( $= 1, 2, 3, 4$ ) the dependent eigenmodes of the electronic part of the renormalized Hamiltonian  $H_0$ , can be written as

$$H_0^{\text{el}} = \sum_{\mathbf{k} \in \text{BZ}} \left( E_{1;\mathbf{k}} a_{1;\mathbf{k}}^\dagger a_{1;\mathbf{k}} + E_{2;\mathbf{k}} a_{2;\mathbf{k}}^\dagger a_{2;\mathbf{k}} + E_{3;\mathbf{k}} a_{3;\mathbf{k}}^\dagger a_{3;\mathbf{k}} + E_{4;\mathbf{k}} a_{4;\mathbf{k}}^\dagger a_{4;\mathbf{k}} \right) \quad (7.5)$$

where the eigenenergies are given by

$$E_{1=2;\mathbf{k}} = \frac{\epsilon_{\mathbf{k}} + \epsilon_{\mathbf{k}+\mathbf{Q}}}{2} \mp W_{\mathbf{k}}, \quad (7.6)$$

$$W_{\mathbf{k}} = \frac{\epsilon_{\mathbf{k}} - \epsilon_{\mathbf{k}+\mathbf{Q}}}{2} + \frac{1}{2} \left( p_{\mathbf{k}}^2 + p_{\mathbf{k}+\mathbf{Q}}^2 + s_{\mathbf{k}}^2 + s_{\mathbf{k}+\mathbf{Q}}^2 \right)$$

for  $\epsilon_{\mathbf{k}} + \epsilon_{\mathbf{k}+\mathbf{Q}} > 0$ , whereas for  $\epsilon_{\mathbf{k}} + \epsilon_{\mathbf{k}+\mathbf{Q}} < 0$  the signs have to be reversed. Note that in (7.6) the sum of the two order parameters squared enter the energies  $E_{\mathbf{k};}$  of (7.6).

In order to derive the renormalization equations, the unitary transformation (2.17) has to be evaluated explicitly. Thereby, also the interaction  $H_1$  has to be expressed in terms of the eigenmodes  $a_{\mathbf{k};}^\dagger$  of  $H_0$ . Moreover, an ansatz for  $X$  has to be made in analogy to what was done in the previous sections. The explicit calculation is found in Ref. 52.

### B. Results and Discussion

For the numerical evaluation of the renormalization equations, we consider a square lattice with  $N = 144$  sites. The temperature is set equal to  $T = 0$ , and a small value of  $\epsilon_0 = 0.1t$  is chosen. For simplicity, we also restrict ourselves to s-wave-like superconducting solutions.

The results are shown in Fig. 9, where the  $\mathbf{k}$ -dependent symmetry breaking fields  $\tilde{s}_{\mathbf{k}}^p$  (black) and  $\tilde{s}_{\mathbf{k}}^s$  (red) for  $\mathbf{k} = (\pi/2, \pi/2)$  are plotted as function of the electron-phonon coupling  $g$ . The coupling  $g$  is restricted to small values  $g = 2t = 0.04$ . As can be seen from Fig. 9, for small

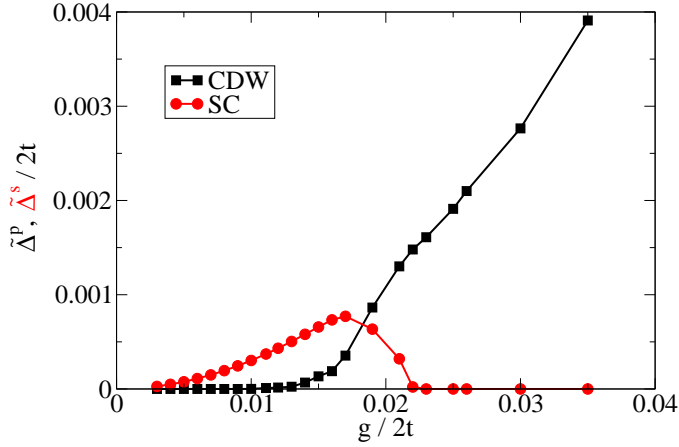


FIG. 9 (Color online) Renormalized values of the Peierls gap  $\tilde{\Delta}_k^P$  (black line) and of the superconducting gap  $\tilde{\Delta}_k^S$  (red line) at wave vector  $k = (\pi/2, \pi/2)$ . A square lattice with 144 lattice sites at half-filling was taken,  $\beta_0 t = 0.1$  and  $T = 0$ .

values of  $g=2t < 0.010$  the system is in a pure superconducting state, i.e. no charge order is present. For small  $g$ , the superconducting gap increases roughly proportional to  $g^2$ . In the intermediate  $g$  range,  $0.010 < g=2t < 0.023$ , a coexistence of both phases is found. The system is in a combined superconducting-charge ordered phase. Here, the  $g$  dependence of  $\tilde{\Delta}_k^S$  is no longer quadratic as in the small  $g$  regime. Instead,  $\tilde{\Delta}_k^S$  reaches a maximum value and drops down to zero with increasing  $g$ . Finally, for  $g=2t > 0.023$  the superconducting phase is completely suppressed and the system is in a pure charge ordered state.

### VIII. SUMMARY

The aim of this contribution was to discuss the basic ideas of a new theoretical approach for many-particle systems which is called projector-based renormalization method (PRM) and its application to a number of non-trivial physical problems. Instead of eliminating high-energy states as in usual renormalization group methods in the PRM high-energy transitions are successively eliminated. Thereby, a unitary transformation is used where all states of the unitary space of the interacting system are kept. In that respect, the PRM is closely related to the similarity transformation introduced by Wilson and Glazek and to Wegner's flow equation method though both approaches start from a continuous formulation of the unitary transformation. The PRM starts from a Hamiltonian which can be decomposed into a solvable unperturbed part and a perturbation,  $H = H_0 + H_1$ , where the latter part induces transitions between the eigenstates of  $H_0$ .

Suppose a renormalized Hamiltonian  $\tilde{H}$  has been constructed which only contains transitions with transition

energies smaller than some given cutoff energy  $\epsilon$ . The Hamiltonian  $\tilde{H}$  can be further renormalized by eliminating all transitions from  $\tilde{H}$ , roughly speaking, the energy shell between the cutoff and a reduced cutoff  $\epsilon'$ , and so on. This is done by a unitary transformation  $H(\epsilon') = e^{X_\epsilon} \tilde{H} e^{-X_\epsilon}$  which guarantees that the eigenspectrum is not changed. The generator of the unitary transformation  $X_\epsilon$  is specified by the condition  $Q_\epsilon H(\epsilon') = 0$  where  $Q_\epsilon$  is the projector on all transitions with energy differences larger than  $\epsilon'$ . The latter condition implies that all transitions from the 'shell' between  $\epsilon$  and  $\epsilon'$  are eliminated and lead to a renormalization of  $H(\epsilon')$ . Note that only the equivalent part  $Q_\epsilon X_\epsilon$  of  $X_\epsilon$  is fixed whereas the orthogonal part  $P_\epsilon X_\epsilon$  can be chosen arbitrarily. Note that this additional freedom can be used in a different way. Whereas in the original version of the PRM the remaining part  $P_\epsilon X_\epsilon$  of  $X_\epsilon$  was set equal to zero for simplicity this part was used in Wegner's flow equation method as the only relevant part when the transformation was performed continuously. In this case, the interaction parameters were chosen to decay exponentially. By proceeding the renormalization up to the final cutoff  $\epsilon = 0$  all transitions induced by  $H_1$  are eliminated. The final renormalized Hamiltonian  $\tilde{H} = H_0, \epsilon = 0$  is diagonal and allows to evaluate in principle any correlation function of physical interest. In particular the one-particle excitations of  $\tilde{H}$  can be considered as quasiparticles of the coupled many-particle system since the eigenspectrum of the original interacting Hamiltonian  $H$  and of  $\tilde{H}$  are in principle the same since both are connected by a unitary transformation.

Note that the present approach has the advantage of formulating the renormalization quite universally. By specifying the unitary transformation of the many-particle system both the PRM and Wegner's flow equation method can be derived from the same basic ideas. However, the stepwise transformation of the PRM has its own merits. Firstly, as was shown in Sec. III C, Sec. VI, and Sec. VII the physical behavior on both sides of a quantum critical point can be described within the same PRM scheme. This seems not the case for the flow equation approach. In particular, by allowing symmetry breaking terms in the 'unperturbed' part  $H_0$ , the transformation of eigenmodes of the Liouville operator  $L_0$  can be followed in each renormalization step. This makes the description of quantum critical points possible. Secondly, in Sec. II B a perturbation theory for  $\tilde{H}$  was given. This allows to evaluate physical properties in perturbation theory. In contrast to a recent perturbation approach on the basis of the flow equation method, in the PRM no equidistant spectrum of  $H_0$  is required.

### Acknowledgments

We would like to acknowledge stimulating and enlightening discussions with A. Mai and J. Schone. This work

was supported by the DFG through the research program SFB 463.

#### APPENDIX A: Example: dimerized and frustrated spin chain

In this appendix we are going to investigate ground-state properties of a dimerized and frustrated spin chain. We apply the projector-based perturbation theory and use expression (2.15) for  $H$  and choose  $\lambda = 0$  right from the beginning. In this case, the interaction  $H_1$  is completely integrated out in one step. The starting Hamiltonian reads

$$\begin{aligned} H &= H_0 + H_1; \\ H_0 &= J \sum_i S_{2i} S_{2i+1}; \\ H_1 &= J \sum_i [S_{2i} S_{2i+1} + (S_{2i} S_{2i+2} + S_{2i+1} S_{2i+3})]; \end{aligned} \quad (\text{A } 1)$$

The model itself is of some physical interest because it can be used to describe some spin-Peierls compounds like  $\text{CuGeO}_3$  or  $\text{TiFeCuBDT}$  (16; 17; 18).

In the following we are interested in the limit of strong dimerization of the model so that we start from isolated dimers as described by  $H_0$ . Every dimer can be in the singlet state or in one of the three degenerated triplet states. Here, the dimer states are energetically separated by the singlet-triplet splitting,  $\epsilon_t - \epsilon_s = J$ . Thus, triplets can be considered as the basic excitations of the system.

Following the ideas of Refs. 14 and 19, the contributions to the perturbation  $H_1$  can be classified according to the number of created or annihilated local triplets,

$$\begin{aligned} H_1 &= \sum_j [T_2(j) + T_1(j) + T_0(j) + T_1(j) + T_2(j)] \end{aligned} \quad (\text{A } 2)$$

The introduced excitation operators  $T_m(j)$  only act on the local dimers with indices  $j$  and  $j+1$ , and create  $m$  local triplets. The  $T_m(j)$  are eigenoperators of the Liouville operator  $L_0$  and the corresponding eigenvalues are  $\epsilon_m = mJ$ . The actual contributions to  $T_0(j)$ ,  $T_1(j)$ , and  $T_2(j)$  are summarized in Table I, and  $T_1(j)$  and  $T_2(j)$  are given by the relation  $T_m(j) = [T_m(j)]^\dagger$ .

In the limit of strong dimerization, Hilbert space sectors with different numbers of triplets in the system are energetically separated because the unperturbed part  $H_0$  of the Hamiltonian (A1) does not change the number of triplets in the system, and the interaction  $H_1$  only leads to modest corrections. Consequently, the evaluation of the effective Hamiltonian (2.15) can be simplified if one concentrates on a Hilbert space sector with a given fixed number of triplets. In the following, actual calculations are presented for the two energetically lowest sectors where the system contains no or only one triplet.

TABLE I Action of the  $T_m(j)$  as used in the calculations. For convenience, the dimer indices of the states are suppressed.

$4T_0(j)$		
$ t^{0,\pm}, s\rangle$	$\rightarrow$	$-J(\alpha - 2\beta)  s, t^{0,\pm}\rangle$
$ t^0, t^\pm\rangle$	$\rightarrow$	$J(\alpha + 2\beta)  t^\pm, t^0\rangle$
$ t^\pm, t^\pm\rangle$	$\rightarrow$	$J(\alpha + 2\beta)  t^\pm, t^\pm\rangle$
$ t^\pm, t^\mp\rangle$	$\rightarrow$	$J(\alpha + 2\beta) \{ t^0, t^0\rangle -  t^\pm, t^\mp\rangle\}$
$ t^0, t^0\rangle$	$\rightarrow$	$J(\alpha + 2\beta) \{ t^+, t^-\rangle +  t^-, t^+\rangle\}$
$4T_1(j)$		
$ s, t^+\rangle,  t^+, s\rangle$	$\rightarrow$	$J\alpha \{ t^+, t^0\rangle -  t^0, t^+\rangle\}$
$ s, t^0\rangle,  t^0, s\rangle$	$\rightarrow$	$J\alpha \{ t^+, t^-\rangle -  t^-, t^+\rangle\}$
$ s, t^-\rangle,  t^-, s\rangle$	$\rightarrow$	$J\alpha \{ t^0, t^-\rangle -  t^-, t^0\rangle\}$
$4T_2(j)$		
$ s, s\rangle$	$\rightarrow$	$J(\alpha - 2\beta) \{ t^+, t^-\rangle +  t^-, t^+\rangle -  t^0, t^0\rangle\}$

The subspace without triplets consists of a single state, i.e. the singlet product state,  $|j_{GS}\rangle = |j_{GS1}\rangle |j_{GS2}\rangle \dots |j_{GSN}\rangle$ . Because the effective Hamiltonian  $H_{\text{eff}}(\lambda=0)$  is obtained from the original Hamiltonian  $H$  by means of a unitary transformation, the ground-state energy can be calculated from

$$\begin{aligned} E_{GS} &= \lim_{\lambda \rightarrow 0} \langle H \rangle = \lim_{\lambda \rightarrow 0} \frac{\text{Tr} H(\lambda=0) e^{-H(\lambda=0)}}{\text{Tr} e^{-H(\lambda=0)}}; \\ &= \langle j_{GS} | H(\lambda=0) | j_{GS} \rangle. \end{aligned}$$

Here  $H(\lambda=0)$  is given by (2.15) where  $P(\lambda=0)H_1 = \sum_j T_0(j)$  and  $Q(\lambda=0)H_1$  is the remaining part of (A2). Using the notation of Ref. 19, one easily finds

$$E_{GS} = NJ \left[ \frac{3}{4} - \frac{3}{32} (2J^2 + O(J_1^3)) \right]; \quad (\text{A } 3)$$

This result agrees with findings of Refs. 14 and 19. Note that higher order terms can easily be calculated by implementing a computer based evaluation algorithm as discussed in Ref. 19 where a cumulant method (15) was applied to the same model.

The case of a single triplet in the system is more complex because a triplet can easily move along the chain. Consequently, it is advantageous to introduce momentum dependent states,

$$|j_k\rangle = \frac{1}{N} \sum_j e^{ikR_j} |j_{GS1}\rangle |j_{GS2}\rangle \dots |t_j\rangle \dots |j_{GSN}\rangle;$$

and the eigenvalues of this Hilbert space sector can be calculated by  $E_k = \lim_{\lambda \rightarrow 0} \langle j_k | H | j_k \rangle$ . We again em-

ploy the useful notation of Ref. 19 and obtain

$$E_k = E_{GS} + J \left( 1 + \frac{3}{16} \left( \frac{2}{a} \right)^2 \frac{1}{4} a^2 \right) \quad (A4)$$

$$J \left( \frac{1}{2} \left( \frac{2}{a} \right) + \frac{1}{4} a^2 \cos(ka) \right)$$

$$\frac{1}{16} J \left( \frac{2}{a} \right)^2 \cos(2ka) + O(a^3):$$

Note that the energy gap of the system can easily be determined from Eq. (A4) by considering the case  $k = 0$ . The  $k$  dependence of  $E_k$  describes the triplet dispersion relation. Furthermore, the calculation can easily be extended to higher orders.

The same model was also studied (14) based on Wegner's own equation method (8) where both ground-state energy and triplet dispersion relation were calculated in high orders. However, for this purpose a set of coupled differential equations had to be integrated so that this approach is restricted to systems with an equidistant eigenvalue spectrum of the unperturbed part  $H_0$  of the Hamiltonian.

## References

- [1] see, for example, H. Q. Lin and J. E. Gubernatis, *Comput. Phys.* **7**, 400 (1993), and references therein.
- [2] K. G. Wilson, *Rev. Mod. Phys.* **47**, 773 (1975); for a recent review see R. Bulla, T. Costi, and T. Puschke, *cond-mat/0701105*.
- [3] W. von der Linden, *Physics Rep.* **220**, 53 (1992).
- [4] S. White, *Phys. Rev. Lett.* **69**, 2863 (1992); for a recent review see P. Schollwöck, *Rev. Mod. Phys.* **77**, 259 (2005).
- [5] W. Metzner and D. Vollhardt, *Phys. Rev. Lett.* **62**, 324 (1989); G. Kotliar and D. Vollhardt, *Physics Today*, March 2004, p. 53; for a review see A. Georges, G. Kotliar, W. Krauth, and M. J. Rozenberg, *Rev. Mod. Phys.* **68**, 13 (1996).
- [6] S. D. Glazek and K. G. Wilson, *Phys. Rev. D* **48**, 5863 (1993).
- [7] S. D. Glazek and K. G. Wilson, *Phys. Rev. D* **49**, 4214 (1994).
- [8] F. Wegner, *Ann. Phys. (Leipzig)* **3**, 77 (1994); see also S. Kehrein, *The Flow Equation Approach to Many-Particle Systems*, Springer Tracts in Modern Physics, Springer-Verlag GmbH, 2006.
- [9] see, for example, J. Zinn-Justin, *Quantum field theory and critical phenomena*, Oxford, Clarendon Press 2002.
- [10] K. W. Becker, A. Hubsch, and T. Sommer, *Phys. Rev. B* **66**, 235115 (2002).
- [11] P. Coleman, *Phys. Rev. B* **29**, 3035 (1984).
- [12] For a review see, for example, P. Fulde, J. Keller, and G. Zwicknagl, in *Solid State Physics*, edited by H. Ehrenreich and D. Tumbull (Academic, San Diego, 1988), Vol. 41, p. 1.
- [13] J. Stein, *J. Stat. Phys.* **88**, 487 (1997).
- [14] C. Knetter and G. S. Uhrig, *Eur. Phys. J. B* **13**, 209 (2000).
- [15] A. Hubsch, M. Voja, and K. W. Becker, *J. Phys.: Condens. Matter* **11**, 8523 (1999).
- [16] J. Riera and A. D. Obry, *Phys. Rev. B* **51**, 16098 (1995).
- [17] G. Castilla, S. Chakravarty, and V. J. Emery, *Phys. Rev. Lett.* **75**, 1823 (1995).
- [18] J. W. Bray, L. V. Interante, I. C. Jacobs, J. C. Bonner, in *Extended Linear Chain Compounds*, edited by J. S. Miller (Plenum Press, New York, 1983), Vol. 3, p. 353.
- [19] S. Sykora, A. Hubsch, and K. W. Becker, *Phys. Rev. B* **70**, 054408 (2004).
- [20] A. Hubsch and K. W. Becker, *Eur. Phys. J. B* **33**, 391 (2003).
- [21] A. Hubsch and K. W. Becker, *Phys. Rev. B* **71**, 155116 (2005).
- [22] A. Hubsch and K. W. Becker, *Eur. Phys. J. B* **52**, 345 (2006).
- [23] S. Sykora, A. Hubsch, K. W. Becker, G. Wellein, and H. Fehske, *Phys. Rev. B* **71**, 045112 (2005).
- [24] P. W. Anderson, *Phys. Rev.* **124**, 41 (1961).
- [25] U. Fano, *Phys. Rev.* **124**, 1866 (1961).
- [26] J. Bardeen, L. N. Cooper, and J. R. Schrieffer, *Phys. Rev.* **108**, 1175 (1957).
- [27] L. N. Cooper, *Phys. Rev.* **104**, 1189 (1956).
- [28] H. Fröhlich, *Proc. R. Soc. London A* **215**, 291 (1952).
- [29] P. Lenz and F. Wegner, *Nucl. Phys. B* **482**, 693 (1996).
- [30] A. Mielke, *Ann. Physik (Leipzig)* **6**, 215 (1997).
- [31] N. N. Bogoliubov, *Nuovo Cim.* **7**, 794 (1958).
- [32] S. Sykora, A. Hubsch, and K. W. Becker, *Eur. Phys. J. B* **51**, 181 (2006).
- [33] S. Sykora, A. Hubsch, and K. W. Becker, *Europhys. Lett.* **76**, 644 (2006).
- [34] P. A. Lee, T. M. Rice, J. W. Serene, L. J. Sham, and J. W. Wilkins, *Comments Condens. Matter Phys.* **12**, 99 (1986).
- [35] R. Franco, M. S. Figueira, M. E. Foglio, *Phys. Rev. B* **66**, 045112 (2002).
- [36] A. Mai, P. V. Nham, A. Hubsch, and K. W. Becker, unpublished.
- [37] Miyake
- [38] J. E. Hirsch and E. Fradkin, *Phys. Rev. B* **27**, 4302 (1983).
- [39] R. H. McKenzie, C. J. Hamer, and D. W. Murray, *Phys. Rev. B* **53**, 9676 (1996).
- [40] H. Zheng, D. Feinberg, and M. Avignon, *Phys. Rev. B* **39**, 9405 (1989).
- [41] L. G. Caron and C. Bourbonnais, *Phys. Rev. B* **29**, 4230 (1984); G. Benfatto, G. Gallavotti, and J. L. Lebowitz, *Helv. Phys. Acta* **68**, 312 (1995).
- [42] A. W. ei e and H. Fehske, *Phys. Rev. B* **58**, 13526 (1998); H. Fehske, M. Holicki, and A. W. ei e, *Advances in Solid State Physics* **40**, 235 (2000).
- [43] R. J. Bursill, R. H. McKenzie, and C. J. Hamer, *Phys. Rev. Lett.* **80**, 5607 (1998).
- [44] E. Jeckelmann, C. Zhang, and S. R. White, *Phys. Rev. B* **60**, 7950-7955 (1999).
- [45] H. Fehske, G. Wellein, G. Hager, A. W. ei e, K. W. Becker, and A. R. Bishop, *Physica B* **359-361**, 699 (2005).
- [46] D. Meyer, A. C. Hewson, and R. Bulla, *Phys. Rev. Lett.* **89**, 196401 (2002).
- [47] R. T. Scalettar, N. E. Bickers, and D. J. Scalapino, *Phys. Rev. B* **40**, 197 (1989).
- [48] F. Marsiglio, *Phys. Rev. B* **42**, 2416 (1990).
- [49] M. Vekic, R. M. Noack, and S. R. White, *Phys. Rev. B* **46**, 271 (1992).

- [50] F. Marsiglio, J. E. Hirsch, Phys. Rev. B 49, 1366 (1994).
- [51] E. Berger, P. Valasek, and W. von der Linden, Phys. Rev. B 52, 4806 (1995).
- [52] S. Sykora, A. Hubsch, and K. W. Becker, to be published.